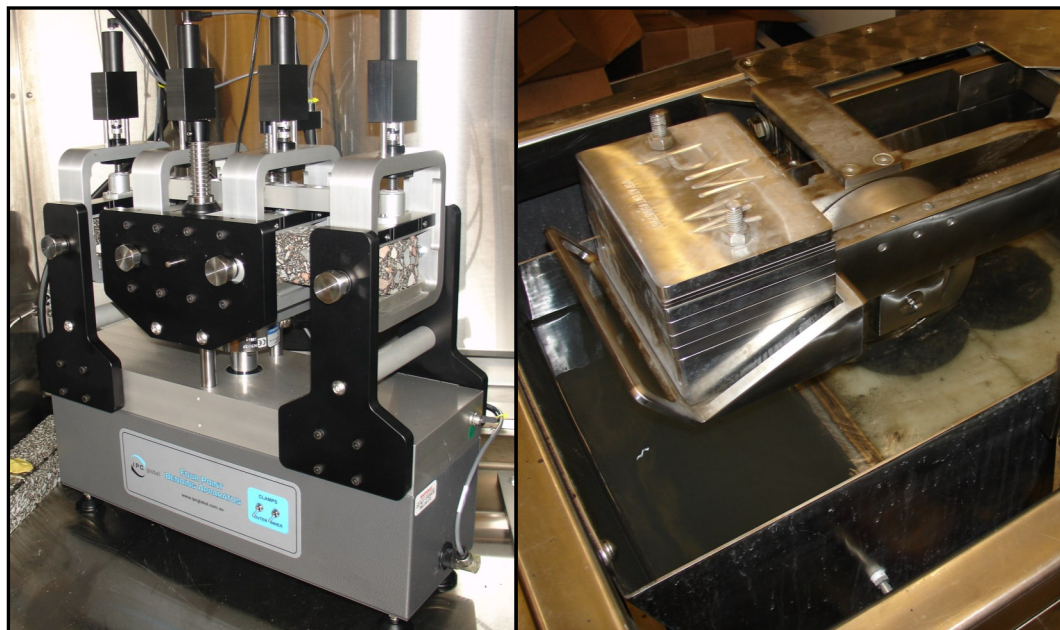**May 2016**

Determination of the Binder Grade and Performance of High Percentage RAP-HMA Mixes

Charles D. Baker, *Governor*

Karyn E. Polito, *Lieutenant Governor*

Stephanie Pollack, *MassDOT Secretary & CEO*

Technical Report Document Page

1. Report No. SPRII-15-57946	2. Government Accession No. n/a	3. Recipient's Catalog No. n/a
4. Title and Subtitle Determination of the Binder Grade and Performance of High Percentage RAP-HMA Mixes	5. Report Date May 2016	
	6. Performing Organization Code n/a	
7. Author(s) Dr. Walaa S. Mogawer, P.E., F.ASCE Mr. Alexander J. Austerman, P.E. Troy Pauli Steve Salmans Jean-Pascal Planche	8. Performing Organization Report No. UMTC-16.02	
9. Performing Organization Name and Address University of Massachusetts Dartmouth Highway Sustainability Research Center (HSRC) 151 Martine Street - Room 131, Fall River, MA 02723	10. Work Unit No. (TRAIS) n/a	
	11. Contract or Grant No. ISA # 57946	
12. Sponsoring Agency Name and Address Massachusetts Department of Transportation Office of Transportation Planning 10 Park Plaza, Suite 4150 Boston, MA 02116	13. Type of Report and Period Covered Final December 2011 to December 2015	
	14. Sponsoring Agency Code n/a	
15. Supplementary Notes n/a		

16. Abstract

This study's purpose was to better understand the effects of incorporating more RAP on the performance of a 9.5 mm Superpave surface course mixture. The performance and workability characteristics of the mixtures were evaluated using two different Warm Mix Asphalt (WMA) technologies and a softer virgin binder grade. The WMA technologies were organic and chemical based.

Mixtures incorporating up to 50% RAP were designed with the same binder content and gradation as the control mixture. At RAP contents beyond 50%, the gradation and binder content of the mixture could not be maintained.

Confirmation of the AASHTO blending charts recommended the use of asphalt binder grades not typically specified in Massachusetts. Binder data indicated that mixtures edged closer to the cracking failure zone as the amount of RAP increased. The use of softer binder and WMA technologies helped to reverse the trends, but the mixtures remained within the onset of cracking zone.

Mixture performance data indicated reduced rutting performance, increased fatigue cracking resistance, and improved mixture workability when the softer binder was utilized. The use of either WMA technology did not significantly impact the rutting or fatigue cracking resistance, but did improve mixture workability.

Using a softer binder or a WMA technology alone did not yield a mixture with the same performance as an all-virgin material mixture. Thus, using higher percentages of RAP in HMA must be carefully developed to reflect variations in individual mixtures based on the properties of RAP, total amount of RAP, available virgin binders, and WMA technologies available. The use of asphalt rejuvenators should be investigated for these types of mixtures to help reuse more of the binder in the RAP.

17. Key Word Reclaimed Asphalt Pavement, Warm Mix Asphalt, Rheology, Performance	18. Distribution Statement No restrictions. This document is available to the public through the sponsoring agent.		
19. Security Classif. (of this report) Unclassified	20. Security Classif. (of this page) Unclassified	21. No. of Pages 90	22. Price n/a

Form DOT F 1700.7 (8-72)   Reproduction of completed page authorized

Blank Page Inserted Intentionally

Determination of the Binder Grade and Performance of High Percentage RAP-HMA Mixes

Final Report

Prepared By:

Professor Walaa S. Mogawer, P.E., F.ASCE
Principal Investigator

Alexander J. Austerman, P.E.
Research Engineer

University of Massachusetts Dartmouth
Highway Sustainability Research Center
151 Martine Street – Room 131
Fall River, MA 02723

and

Troy Pauli
Principal Scientist

Steve Salmans
Senior Scientist

Jean-Pascal Planche
Vice-President

Western Research Institute (WRI)
3474 N. 3rd Street
Laramie, WY 82072

Prepared For:

Massachusetts Department of Transportation
Office of Transportation Planning
10 Park Plaza, Suite 4150
Boston, MA 02116

May 2016

Blank Page Inserted Intentionally

Acknowledgements

Disclaimer

Blank Page Inserted Intentionally

Executive Summary

This study of Determination of the Binder Grade and Performance of High Percentage RAP-HMA Mixes was undertaken as part of the Massachusetts Department of Transportation Research Program. This program is funded with Federal Highway Administration (FHWA) Statewide Planning and Research (SPR) funds. Through this program, applied research is conducted on topics of importance to the Commonwealth of Massachusetts transportation agencies.

The purpose of this project was to determine the appropriate binder grade for hot mix asphalt (HMA) mixtures containing varying high percentages of reclaimed asphalt pavement (RAP). For this project, high percentage RAP was defined as equal to or greater than 25%. Mixtures with up to 75% RAP content were attempted; however, only mixtures with up to 50% RAP were able to be designed and evaluated. This is due, in part, to the fact that the 75% RAP content mixture required fractionating the RAP to individual sizes. Since RAP fractionation was not required for the rest of the mixtures, the 75% RAP mixture was eliminated from the study. Testing of the remaining HMA mixtures was conducted in order to evaluate the effect of the higher percentage RAP on their performance. The performance aspects that were measured were mixture durability, stiffness, low temperature cracking characteristics, and fatigue cracking resistance.

Since the binder in RAP has been exposed to the elements for many years, it has experienced significant aging compared to a virgin binder. Therefore, it has different characteristics and quality. The aged binder in RAP causes an increase in mixture stiffness in mixtures high in RAP content. Mixture stiffness then leads to a reduced workability in high RAP mixtures. Thus, Warm Mix Asphalt (WMA) technologies have been utilized to help improve the workability and compactability of HMA mixes that incorporate RAP. Two of these technologies were evaluated in this study in order to determine their effects on mixture workability. Furthermore, the effects of these two WMA technologies and the use of a softer binder were investigated using rheology space diagrams. Diagramming was performed in order to determine the capabilities of either WMA technologies or a softer virgin binder to mitigate the effect of the aged RAP binder in the overall mixture.

Finally, the degree of blending (commingling) between the RAP binder and the virgin binder was evaluated in order to determine if the RAP binder fully contributed all of its binder to the final mixture.

Based on the data collected and analyzed for this study, the following conclusions were made:

1. Superpave 9.5 mm mixtures could be designed with up to 50% RAP with the same binder content and gradation as a control mixture with 0% RAP. Mixtures with RAP contents above 50% were not included in this study because they could not be designed to meet the same mixture requirements.

2. Increased RAP content led to a binder in the mixture that was more aged than the binder in the PG64-28 control mixture. The use of a PG52-34 binder (softer binder) or a WMA technology decreased the degree of aging, with the PG52-34 binder being more effective than the WMA technologies.

3. The results from a Black-Space rheology diagram showed that the control mixture and all RAP mixtures designed with the PG64-28 binder fell in the area of the "onset cracking zone." That is, the mixtures edged closer to the failure zone as the amount of RAP increased. The use of the softer PG52-34 binder or a WMA technology improved the cracking performance of the 35% and the 50% RAP mixtures; however, both mixtures still fell within the onset of cracking zone.

4. The Hamburg wheel tracking device (HWTD) mixture test illustrated that the use of the softer PG52-34 binder in the mixtures containing 35% and 50% RAP contents led to a mixture that was less stiff than the PG64-28 control mixture. This agreed with the binder data resulting from the rheology space diagrams. The WMA technologies did not reduce the stiffness of the mixtures significantly; this finding also agreed with the binder data.

5. The control mixture and all RAP mixtures designed with the PG64-28 binder did not show a significant difference in fatigue cracking resistance. The use of the softer PG52-34 binder did increase fatigue cracking resistance. This finding was consistent with the data collected from the rheology space diagrams, as well as the data from the HWTD mixture data, both of which indicated less mixture stiffness. The use of the WMA technology generally decreased fatigue cracking resistance compared to the other mixtures, although the mixture's significance is most clearly seen when compared to the PG52-34 mixtures.

6. Increasing the amount of RAP in the mixture decreased mixture workability. Although the use of the softer PG52-34 binder or a WMA technology indicated improved workability, their use must be balanced so that other performance indicators are not degraded.

7. Using the softer PG52-34 binder or a WMA technology alone yielded a mixture with more rutting susceptibility than the PG64-28 control mixture. Furthermore, rheology tests showed that the softer binder, or a WMA technology, would not result in a mixture with more resistance to aging. Thus, the use of higher percentages of RAP in HMA must be carefully developed for each specific mixture based on the properties of the RAP, the amount of RAP, the available virgin binders, and the available WMA technologies.

8. Analysis of the reduced binder contribution from the RAP suggested that the actual contribution of the RAP binder may not be a fixed value; hence, a state department of transportation agency cannot give a fixed credit for the binder in the RAP based solely on its contents.

Table of Contents

Blank Page Inserted Intentionally

List of Tables

Blank Page Inserted Intentionally

List of Figures

Blank Page Inserted Intentionally

List of Acronyms

AASHTO	American Association of State Highway and Transportation Officials
AFM	Atomic Force Microscopic
AWD	Asphalt Workability Device
DOT	Department of Transportation
CAM	Christensen-Anderson Model
DSR	Dynamic Shear Rheometer
ESALs	Equivalent Single Axle Loads
HMA	Hot Mix Asphalt
HSRC	Highway Sustainability Research Center
HWTD	Hamburg Wheel Tracking Device
MassDOT	Massachusetts Department of Transportation
NCHRP	National Cooperative Highway Research Program
NEAUPG	Northeast Asphalt User Producer Group
NMAS	Nominal Maximum Aggregate Size
PAV	Pressure Aging Vessel
PG	Performance Grade
PGAB	Performance Grade Asphalt Binder
RAP	Reclaimed Asphalt Pavement
RTFO	Rolling Thin Film Oven
SGC	Superpave Gyratory Compactor
SIP	Stripping Inflection Point
SPR	Statewide Planning and Research
VFA	Voids Filled with Asphalt
VMA	Voids in Mineral Aggregate
WMA	Warm Mix Asphalt

Blank Page Inserted Intentionally

1.0 Introduction and Methodology

This study of Determination of the Binder Grade and Performance of High Percentage RAP-HMA Mixes was undertaken as part of the Massachusetts Department of Transportation Research Program. This program is funded with Federal Highway Administration (FHWA) Statewide Planning and Research (SPR) funds. Through this program, applied research is conducted on topics of importance to the Commonwealth of Massachusetts transportation agencies.

The price increase of oil has led to a dramatic increase in the cost of asphalt binder. Consequently, the expense for Hot Mix Asphalt (HMA) mixtures has increased substantially. To offset this rise in cost, government and private HMA agencies have been searching for methods to reduce the price of HMA mixtures. One option that has been utilized is to increase the amount of Recycled Asphalt Pavement (RAP) allowed in the HMA. Increasing RAP allows for a greater volume of the liquid asphalt binder in the HMA to come from the RAP, thereby decreasing the amount of virgin liquid asphalt binder required for the final mix. Thus, increasing the RAP could potentially save a significant amount of money for the agency in material costs.

MassDOT specification allows 15% RAP in its HMA mixtures. However, many HMA plants are now able to incorporate higher percentages of RAP into the HMA without a negative impact on the mixture's production or the environment in which it is utilized. Using RAP at higher percentages is viable due to the fact that there have been significant improvements made to the equipment used in its processing and handling; these improvements have thus yielded more efficient systems for crushing and fractionating the RAP into more useable forms. As a result, quality HMA can be produced with higher RAP contents than have typically been specified by state and municipal agencies. Several states are currently allowing higher than 10% RAP in their surface course mixtures. For example, New York allows 20% RAP in their surface mixtures, while other states like Arkansas and Minnesota allow over 35% RAP (*1*).

The liquid asphalt from RAP is stiff because it has already been aged. Since the stiffness of the liquid asphalt impacts the performance of HMA mixtures (such as enabling premature cracking and creating less compactable mixtures), it is essential to use a virgin binder that will lead to a target Performance Grade Asphalt Binder (PGAB) when blended with the liquid asphalt from RAP. The American Association of State Highway and Transportation Officials (AASHTO) Specification M323, "Superpave Volumetric Mix Design," (*2*) presents a procedure based on the research results of the National Cooperative Highway Research Program (NCHRP) Project 9-12 "Incorporation of Reclaimed Asphalt Pavement in the Superpave System" (*3*) that can assist in selecting the proper PGAB for high percentages of RAP. However, the procedure generally leads to the use of a softer binder. Recent studies have shown that the use of a PG64-XX can lead to the same performance as a softer PG58-XX, or even PG52-XX (*4*).

The purpose of this project was to determine the binder grade of HMA mixtures containing varying high percentages of RAP (for this project, high percentage RAP is defined as equal to or greater than 25%). Also, testing (durability, stiffness, low temperature cracking characteristics, and fatigue cracking resistance) of these HMA mixtures was conducted in order to evaluate the effect of the higher percentage RAP on the performance of HMA mixes.

Since the aged binder in RAP causes an increase in mix stiffness, the resultant HMA mixes tend to be less workable. Warm Mix Asphalt (WMA) technologies have been utilized to help improve the workability and compactability of HMA mixes that incorporate RAP. Two of these technologies were evaluated in this study in order to determine their effects on mixture workability.

Finally, the degree of blending (commingling) between the RAP binder and the added virgin binder was evaluated in an attempt to determine if the RAP binder does, in fact, fully contribute all of its binder to the final mixture.

The objectives of this project are listed below:

1. Prepare a typical Superpave mix using 0%, 15%, 35%, and 75% RAP with one aggregate source, one RAP source, and two Performance Grade Asphalt Binders.

2. Measure the degree of blending between the aged asphalt liquid and the added virgin liquid.

3. Evaluate the effect of WMA on the workability of HMA with high percentages of RAP.

4. Evaluate and compare the performance of each mix in terms of its durability, fatigue cracking resistance, and stiffness.

In order to fulfill the objectives of this study, an experimental plan was proposed as shown in Figures 1.1 and 1.2. However, over the course of the project, several new methodologies emerged that helped the industry better evaluate the effect of the aged RAP binder on the rheology characteristics of the resulting binder. In order to evaluate the quality of the resultant binder in a high RAP mixture, the new methodology of chemical testing was attempted. This test could also be used to evaluate the degree of blending between aged and virgin binders. All tests will be further explained in the sections detailing binder testing and mixture performance testing.
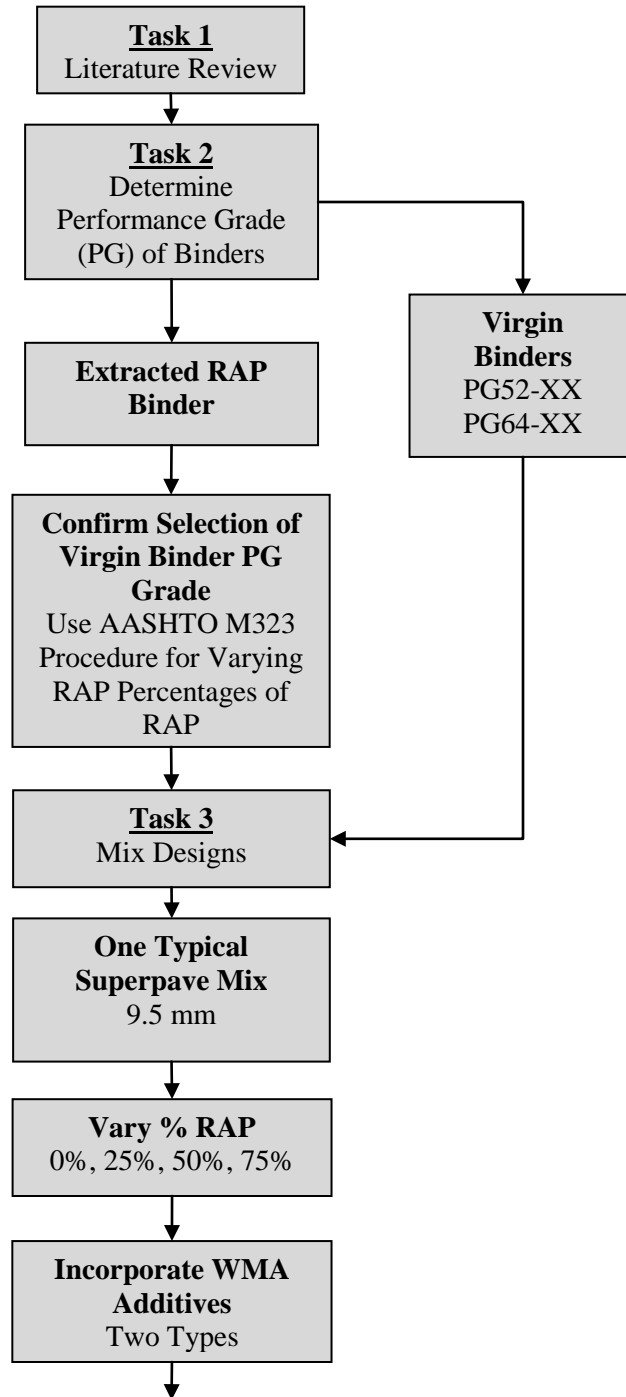
Figure 1.1: Experimental Plan (Part I)
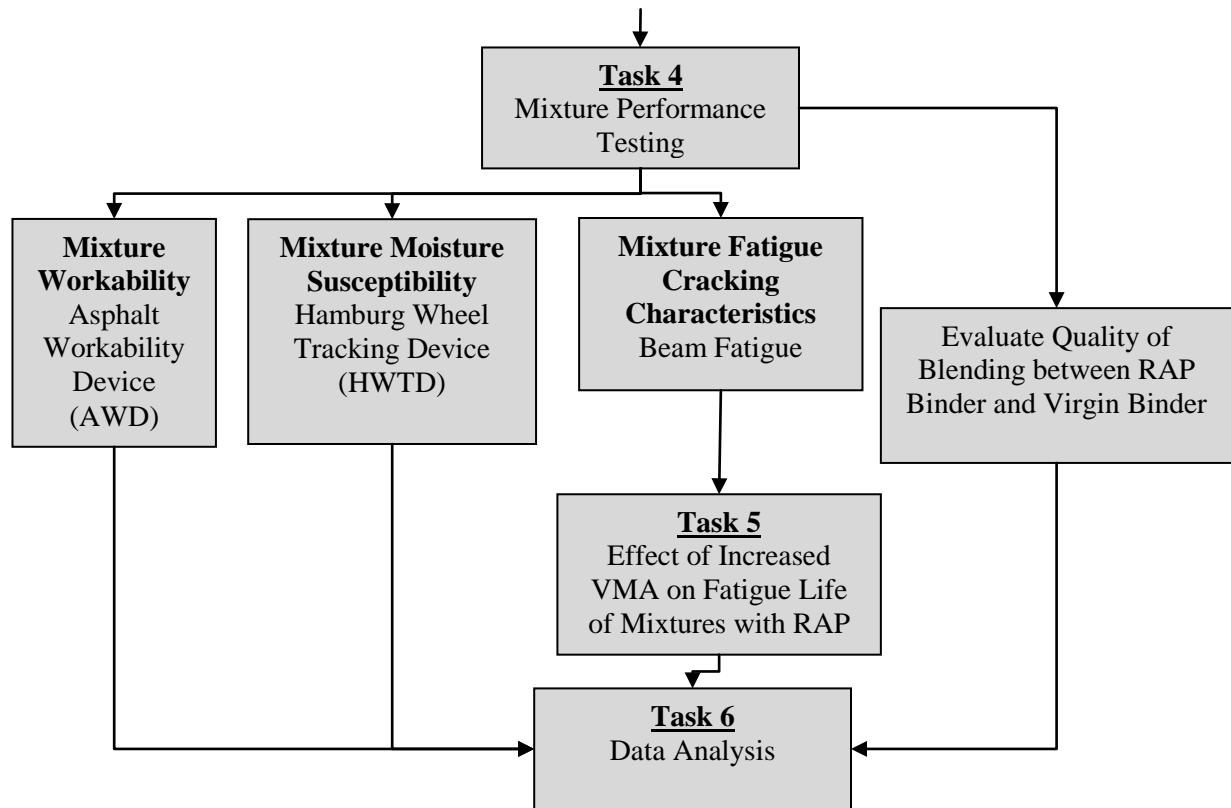
Figure 1.2: Experimental Plan (Part II)

2.0 Materials

In this section, the materials utilized for this study are described. These materials include the asphalt binder, aggregates, and WMA technologies.

2.1 Asphalt Binder

For this study, two different asphalt binders were utilized. The binders consisted of a PG64-28, which is typically specified in the Northeast, and a PG52-34. The PG64-28 was obtained from Aggregate Industries, and the PG52-34 was obtained from All States Asphalt.

The PG grade of each binder was verified in accordance with AASHTO M320 "Standard Specification for Performance-Graded Asphalt Binder" (*2*), and the mixing and compaction temperatures were determined based on each binder's viscosity. The results of these verifications and tests are shown in Table 2.1.

Table 2.1: Asphalt Binder Information

Binder	Continuous Grade	Performance Grade (PG)	Mixing Temperature Range	Compaction Temperature Range
PG64-28	64.4-28.1	PG64-28	162–158°C (324–316°F)	152–146°C (306–295°F)
PG52-34	54.8-34.5	PG52-34	147–139°C (296–283°F)	127–115°C (260–239°F)

2.2 Aggregates

The aggregates utilized were from a crushed stone source in Wrentham, Massachusetts. The two aggregate stockpiles that were obtained consisted of the following: 9.5 mm crushed stone and stone dust. Each aggregate stockpile was tested to determine its properties. These properties are shown in Table 2.2. Sieve analysis was completed in accordance with two methods: the AASHTO test method T11, also known as the "Standard Method of Test for Materials Finer Than 75-µm (No. 200) Sieve in Mineral Aggregates by Washing," and T27, also called the "Standard Method of Test for Sieve Analysis of Fine and Coarse Aggregates" (*2*).

Table 2.2: Aggregate Properties

Sieve Size	9.5 mm	Stone Dust
19.0 mm	100	100
12.5 mm	99.4	100
9.5 mm	93.8	100
4.75 mm	29.7	99.7
2.36 mm	5.2	83.7
1.18 mm	2.8	57.1
0.600 mm	2.3	38.6
0.300 mm	2.1	24.9
0.150 mm	1.8	15.9
0.075 mm	1.5	10.9

2.3 Reclaimed Asphalt Pavement (RAP)

RAP was obtained from the same contractor as the aggregates. The RAP stockpile was fractionated in the laboratory in order to meet the mixture gradation requirements for this study. The binder content of the RAP material was determined to be 5.6% using the ignition oven test method, in accordance with AASHTO T308, "Determining the Asphalt Binder Content of Hot Mix Asphalt (HMA) by the Ignition Method" (*2*). The aggregates in the RAP that remained after the ignition were tested in order to determine their properties. These properties are also shown in Table 2.3. The RAP binder was extracted and recovered in accordance with AASHTO T164, or the "Standard Method of Test for Quantitative Extraction of Asphalt Binder from Hot Mix Asphalt (HMA)," as well as AASHTO T170, the "Standard Method of Test for Recovery of Asphalt Binder from Solution by Abson Method" (*2*). As shown in Table 2.3, the continuous and performance grade of the recovered RAP binder was determined in accordance with AASHTO R29, "Grading or Verifying the Performance Grade of an Asphalt Binder" and AASHTO M320, "Standard Specification for Performance-Graded Asphalt Binder" (*2*).

Table 2.3: RAP Properties

Sieve Size	RAP Aggregates Post Ignition
9.5 mm	100
4.75 mm	76.8
2.36 mm	57.6
1.18 mm	43.3
0.600 mm	31.1
0.300 mm	19.8
0.150 mm	12.1
0.075 mm	8.3
RAP Binder Content, % =	5.6%
RAP Binder Continuous Grade =	82.0–21.8
RAP Binder Performance Grade =	PG82-16

2.4 Warm Mix Asphalt (WMA)Technologies

Two different WMA technologies were utilized for this study. According to the MassDOT technical representative, the technologies were chosen from the Northeast Asphalt User Producer Group (NEAUPG) approved list. From the approved NEAUPG list, the MassDOT technical representative approved the use of an organic-based WMA technology (1.0% SonneWarmix by weight of binder) and a chemical-based technology (0.5% Evotherm P15 by weight of binder). The reduced mixing and compaction temperatures for using each WMA with the PG64-28 were 135°C (275°F) and 125°C (256°F), respectively. Similarly, the reduced mixing and compaction temperatures for using each WMA with the PG52-34 were 118°C (245°F) and 105°C (220°F), respectively, based on the manufacturers' recommendations.

Blank Page Inserted Intentionally

3.0 Mixture Design

The target gradation for the mixtures utilized in this study is shown in Table 3.1. The target gradation was developed to meet the requirements for a 9.5 mm Superpave mixture in accordance with AASHTO M323, "Superpave Volumetric Mix Design," as well as AASHTO R35, "Superpave Volumetric Design for Hot Mix Asphalt" (*2*). The design Equivalent Single Axle Loads (ESALs) for this project was selected as 0.3 to <3 million, which is consistent with surface course mixtures in New England. The design Superpave gyratory compactive effort for this ESALs level was Ndesign = 75 gyrations.

Table 3.1: Target Mixture Gradation and Specification

Sieve Size	Sieve Size (mm)	Target Gradation for All Mixtures	Superpave 9.5 mm Specification
1/2"	12.5 mm	100	100 min
3/8"	9.5 mm	98	90–100
No. 4	4.75 mm	85	90 max
No. 8	2.36 mm	58	32–67
No. 16	1.18 mm	42	-
No. 30	0.600 mm	27	-
No. 50	0.300 mm	15	-
No. 100	0.150 mm	9	-
No. 200	0.075 mm	6	2–10
Binder Content =		6.5%	-

First, the control mixtures utilizing all virgin materials were designed utilizing the PG64-28 binder and the PG52-34 binder for comparison purposes. RAP was then incorporated to replace a portion of the virgin materials in the control mixtures. RAP was added to replace a percentage of the mixture aggregates with RAP aggregates (25%, 50%, and 75%). The aggregate gradations for the control and RAP mixtures were identical. Because the gradations were identical for the mixtures developed, mixture design verifications were performed for the RAP mixtures. These verifications attended to RAP both with WMA and without WMA in order to reflect the design binder content determined for the control mixture. Verifications were completed assuming 100% contribution of the RAP binder.

To incorporate the RAP into the mixtures, a procedure that was used in a prior study utilizing similar materials was followed (*5*). This procedure was used in order to eliminate moisture in the RAP stockpile material and to optimize the blending between the aged and virgin binders in the mixture. The procedural steps are listed below:

1. The RAP was air dried until a constant mass was achieved, which typically took three to five days.

2. The RAP was further dried for two days at 60ºC (140ºF).

3. The RAP was added to heated aggregate during the mixing process two hours prior to adding the binder.

During initial verifications of the 75% RAP mixture, it was noted that the volumetric properties were very different from the control mixture. Forensic testing indicated that the RAP fractionating required for the 75% RAP mixture yielded a mixture that had a different binder content and gradation than that of the control. Thus, no further testing was completed on this mixture, since it could not be compared with any of the other mixtures. Instead, RAP contents of 15% and 35% were added to the study. A 50% RAP mixture was determined to be the upper limit that could be utilized without requiring further fractionation of the RAP. In total, 30 mixture designs/verifications were completed, as shown in Table 3.2.

The results of the mixture designs and verifications for each of the 30 mixtures are shown in Appendix 9-1. Generally, the volumetric data shows an increase in air voids as the percentage of RAP is increased. This increase may indicate that there is not 100% contribution of the RAP binder, which then leads to a mixture with less effective asphalt binder content. Another possible explanation is that good blending took place, resulting in a stiff binder, which then led to a mixture that was difficult to compact. Additionally, certain WMA mixtures exhibited high air voids; these voids may indicate that the compaction temperature reductions utilized were too great, because they led to a stiff mixture that was more difficult to compact.

Based on the mixture design and verifications, mixtures were selected for further analysis in terms of both binder and mixture performance testing. These mixtures were selected in an attempt to address the variables of the study, which included RAP content, different virgin binder grades, and different WMA technologies. The mixtures for further analysis are shown in Table 3.3.

Table 3.2: Mixture Design and Verifications

Virgin Binder	% RAP	WMA Additive
PG64-28	0%	HMA – None
		SonneWarmix
		Evotherm P15
	15%	HMA – None
		SonneWarmix
		Evotherm P15
	25%	HMA – None
		SonneWarmix
		Evotherm P15
	35%	HMA – None
		SonneWarmix
		Evotherm P15
	50%	HMA – None
		SonneWarmix
		Evotherm P15
PG52-34	0%	HMA – None
		SonneWarmix
		Evotherm P15
	15%	HMA – None
		SonneWarmix
		Evotherm P15
	25%	HMA – None
		SonneWarmix
		Evotherm P15
	35%	HMA – None
		SonneWarmix
		Evotherm P15
	50%	HMA – None
		SonneWarmix
		Evotherm P15

Table 3.3: Mixture Selected for Evaluation

Binder	% RAP	WMA Additive
PG64-28	0% – Control	NONE
	15%	NONE
	25%	NONE
	35%	NONE
	50%	NONE
PG64-28	35%	SonneWarmix & Evotherm P15
	50%	SonneWarmix & Evotherm P15
PG52-34	35%	SonneWarmix & Evotherm P15
	50%	SonneWarmix & Evotherm P15

4.0 Binder Testing

This section outlines the binder testing corresponding to the nine mixtures selected for evaluation, as previously shown in Table 3.3.

4.1 AASHTO M323 Blending Charts

As outlined in the experimental plan, one task of this project was to confirm the selection of the virgin binder grade using the methodology in AASHTO M323 (*2*). Based on the extracted RAP properties, the virgin binder grade required for each percentage of RAP is shown in Table 4.1 (assuming a PG64-28 is the desired final PG grade of the binder in the mixture). The grades determined vary from the grades commonly utilized and specified in Massachusetts.

Table 4.1: Blending Chart Confirmation by AASHTO M323

% RAP	Virgin Grade Required by AASHTO M323
15%	PG64-34
25%	PG58-34
35%	PG58-34
50%	PG46-40

4.2 Black Space Diagram and CAM Model

Recently, G* and δ have also been used to generate a rheological plot commonly referred to as a Black Space Diagram. Researchers have illustrated the use of a Black Space Diagram to evaluate the changes in binder rheology due to aging (*6, 7*). Another analysis that can be used to evaluate these changes is the Christensen-Anderson Model (CAM). The two methodologies were the focus of this study in order to understand the impact of the aged RAP binder at varying percentages.

4.2.1 Black Space Diagram and the Glover-Rowe Damage Parameter

Figure 4.1 illustrates a Black Space diagram that shows the current performance grade (PG) parameter for fatigue cracking (G*sinδ), in addition to a new Black Space function defined by a new parameter, named the Glover-Rowe parameter, in the form of $G^*(\cos \delta)^2/(\sin\delta)$ (*7*). This parameter was developed based on the Glover fatigue cracking parameter, $G'/(\eta'/G')$, which was found to have a high correlation with the ductility of the asphalt binder (*8*). Asphalt ductility is determined from the intermediate temperature determined during dynamic shear rheometer (DSR) testing. The advantage of this Glover-Rowe parameter is that as long as the test frequency (ω) is known, variables G* and δ can be plotted to create a

damage curve in black space. Based on the work of Anderson et al. (*7*) and Rowe (*9*), preliminary thresholds have been proposed to determine when non-load associated cracking, specifically block cracking, may begin (Damage Onset) and when there will be definite cracking problems (Significant Cracking). A typical cause of block cracking is the inability of the asphalt binder to expand and contract with temperature cycles because of the constant aging of the asphalt binder. These thresholds have $G^*(\cos \delta)^2/(\sin\delta)$ values of 180 kPa and 450 kPa, respectively, when tested at 15°C (59°F) and a loading frequency of 0.005 radians/sec.
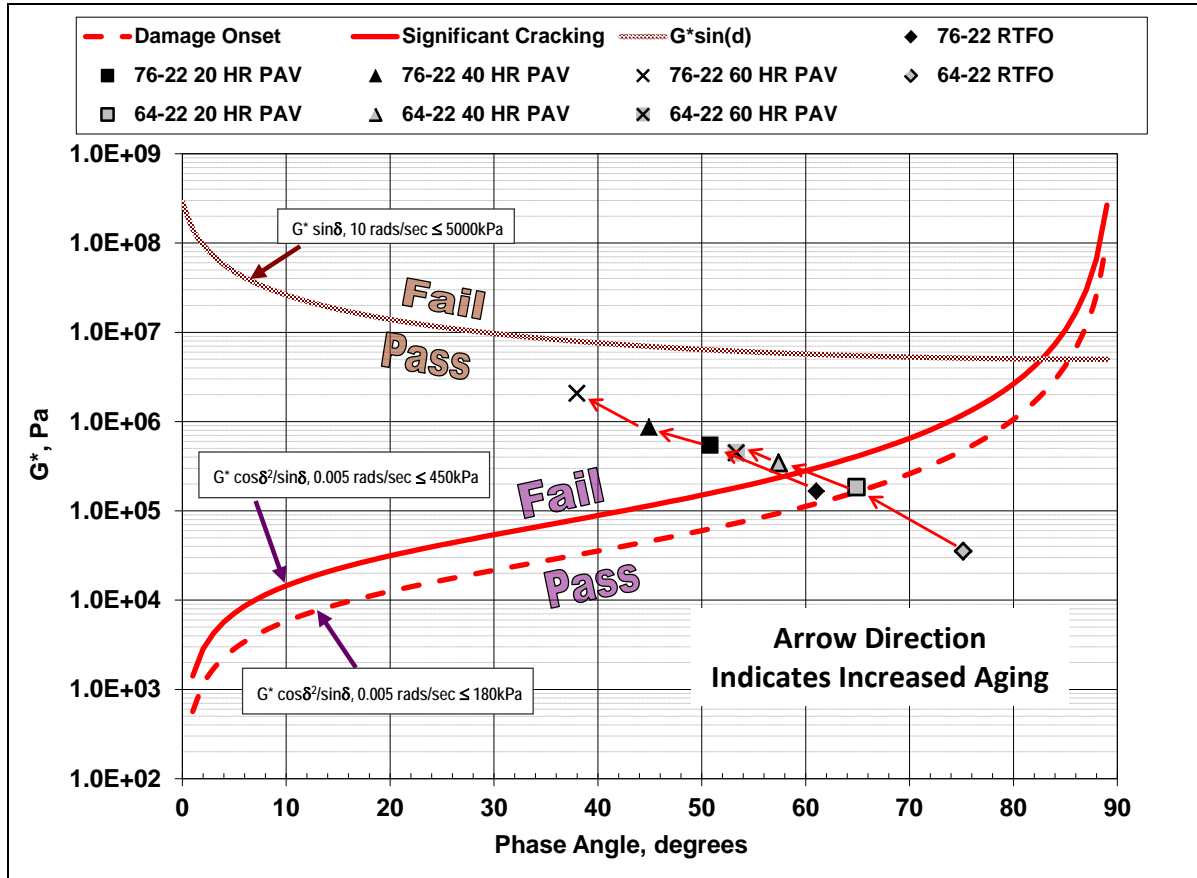
Figure 4.1: PAV-aged Binders Passing through the Glover-Rowe Damage Zone

Similar to the work described by Anderson et al. (*7*), Figure 4.1 illustrates data for two different binders (PG64-22 and PG76-22) that were aged in a pressure aging vessel (PAV) for 0, 20, 40, and 80 hours. The PAV aging was done after all binders were short-term aged in a rolling thin film oven (RTFO). The purpose of the longer PAV aging times was to create a more highly aged sample in the laboratory. Using the new Glover-Rowe parameter and presenting the data in Figure 4.1, the RTFO aging for each binder started at the lower right location in the Black Space diagram; each additional aging period caused the rheological properties to move to the upper left of the diagram (demonstrating an increase in stiffness and a reduced phase angle for each binder). It should be noted that even after 60 hours of

14

PAV aging, the asphalt binders still "pass" the current G*sinδ Superpave specification. For extracted and recovered binders from high RAP content mixtures with consequently higher amounts of aged binder in a mixture, binder testing data is expected to follow the same trend as illustrated in Figure 4.1. The rheological response shows a trend to move toward the upper left of the Black Space diagram. Daniel (*10*) confirmed this trend on both extracted and recovered asphalt binders from plant-produced mixtures in Vermont. The trend in the Black Space diagram indicated that as RAP percentage increased for the same mixture, the G* and δ data migrated from the lower right to the upper left of the Black Space. Therefore, it is expected in this study that as the amount of RAP increases, the same trend would result. This would also be a good indication that good blending is occurring between the aged and virgin binders.

For the mixtures in this study, the binder from volumetric specimens was extracted and recovered. G* master curves were also measured and utilized in order to evaluate the overall stiffness properties of the asphalt binders, as well as their relative aging characteristics. Prior to actual testing of each recovered asphalt binder, the DSR was run in an oscillatory mode in order to ensure that the asphalt binder sample would be tested in the linear region at the respective test temperature. The following test temperatures were used in the following order: 10°, 22°, 34°, and 46°C. The following range of loading frequencies were utilized to cover two decades of loading times and were conducted in the following order: 100, 62.8, 31.4, 10, 6.28, 3.14, 1.0, 0.63, 0.1, and 0.063 radians/sec. The Glover-Rowe parameter was determined by curve shifting and not measured directly at 0.005 radians/second at 15°C.

As indicated in Figures 4.2 to 4.4, the use of the PG64-28 showed that the control mixtures and the RAP mixtures fell in the onset of cracking zone in the Black Space diagram. It should be noted that the mixtures edged closer to the failure zone, in terms of cracking due to aging, as the amount of RAP increased. The use of softer binder and WMA helped reverse the trends for the 35% and the 50% RAP mixtures; nevertheless, both mixtures were still in the onset of cracking zone.
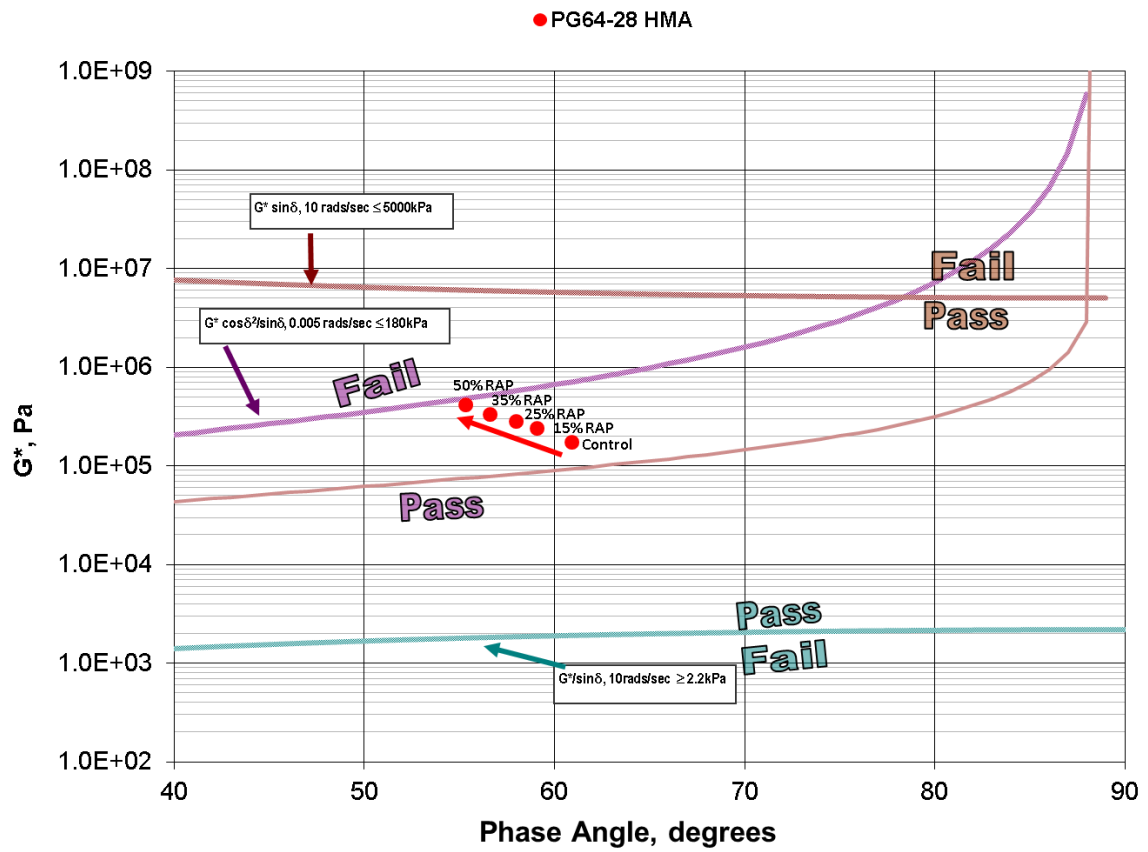
Figure 4.2: Black Space Diagram for Extracted Mixtures Binders, PG64-28 HMA
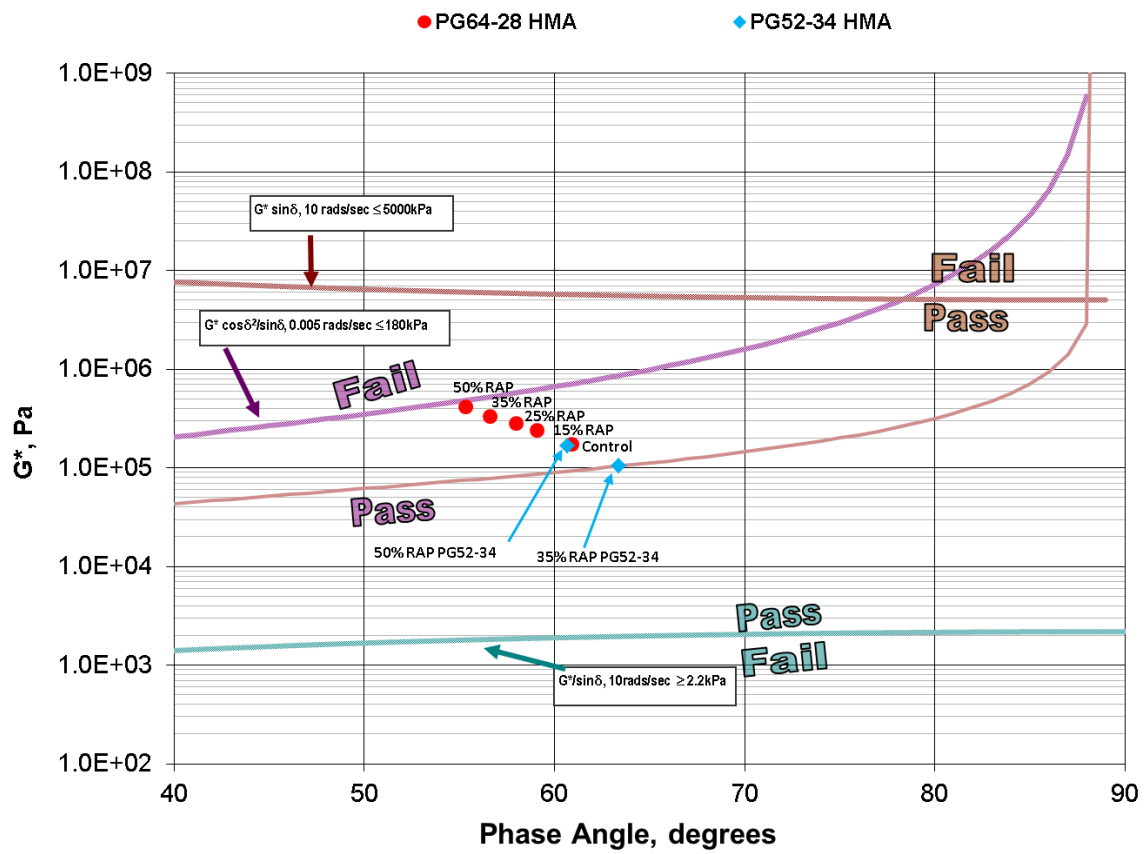
Figure 4.3: Black Space Diagram for Extracted Mixtures Binders, PG52-34HMA
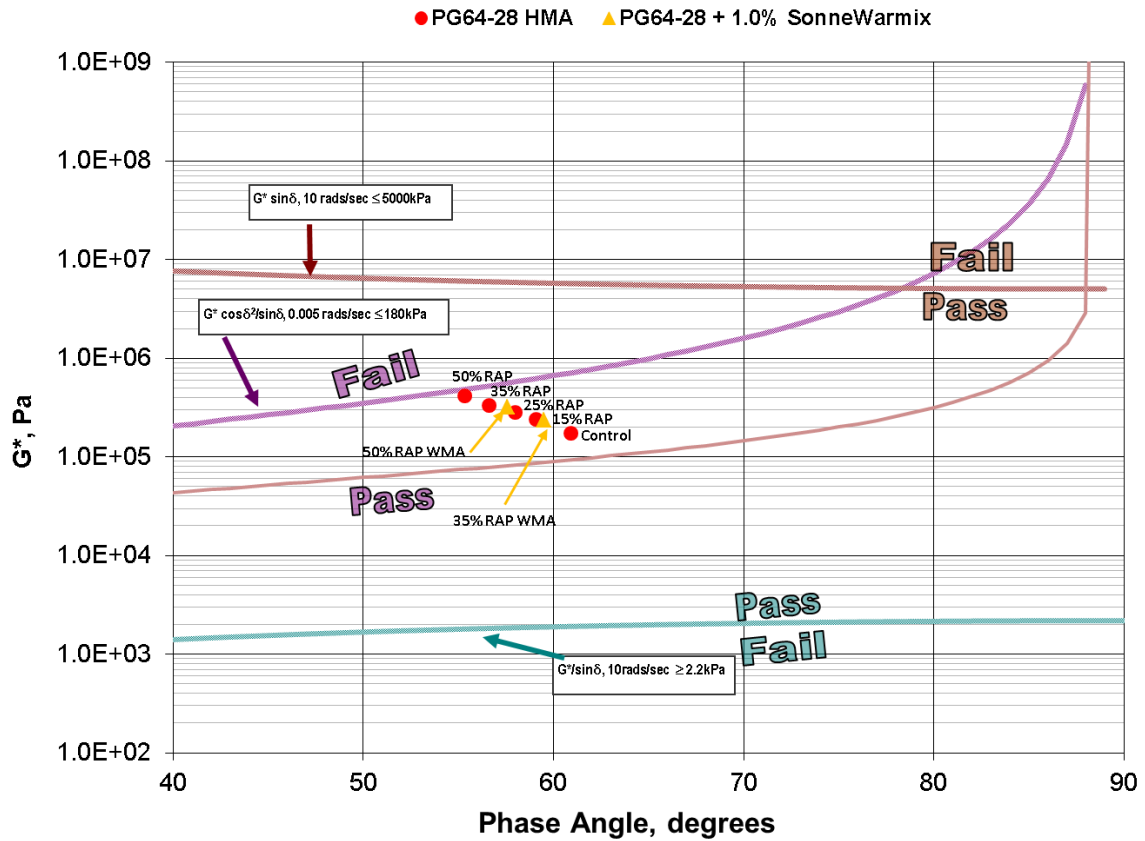
Figure 4.4: Black Space Diagram for Extracted Mixtures Binders- PG64-28 WMA

4.2.2 Christensen-Anderson Model (CAM) Master Curve Parameters

Another tool that can be used to investigate the effect of incorporating high RAP contents on the rheological properties of the resultant binders is to use traditional rheological master curves of G* versus loading frequency. The Christensen-Anderson Model (CAM) is a very useful tool because the master curve parameters (ω_o, R, and T_d) have specific physical significance. The Cross-over Frequency, ω_o, is a measure of the overall hardness of the binder. As this frequency increases, the hardness of the binder decreases, which is desirable for rejuvenated binders. The Rheological Index, R-value, is an indicator of the rheological type. It is defined as the difference between the log of the glassy modulus and the log of the dynamic modulus at the crossover frequency. As R-value increases, the master curve becomes flatter, indicating a more gradual transition from elastic behavior to steady-state flow. Normally, R-value is higher for oxidized asphalt. Accordingly, the R-value is expected to increase with oxidization. Therefore, for rejuvenators to be effective, the R-value for the overall aged binder plus virgin binder should decrease. Figure 4.5 shows the parameters used to define the shape of the binder master curve.
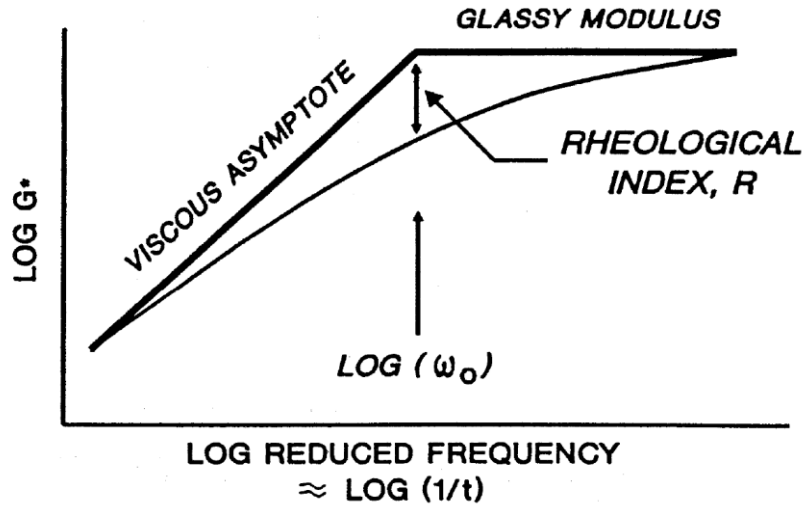
Figure 4.5: Functional Form of Christensen-Anderson Asphalt Binder Master Curve Model (*11*)

Figure 4.6 shows the ω_o and R-value for the same test data presented earlier in Figure 4.1. In this case, ω_o and R-value are plotted in their own space (ω_o – R-value Space). The PG64-22 and PG76-22 asphalt binders migrate from the upper left to the lower right of the ω_o – R-value Space as the magnitude of aging increases. The same trend can be expected as the RAP content of the asphalt mixture increases.

The results and subsequent analyses of the master curve test indicate that G* and δ, as well as the functional form of the master curve itself (ω_o and R-value), can be used to evaluate aging in an asphalt binder. Since aging can be clearly identified using this method, it is hypothesized that the same testing and evaluative procedures can be used to determine the effectiveness of incorporating more RAP, which in turn increases the amount of aged binder in the mix.

Testing was completed as described for development of the Black Space diagrams. The data was used to determine ω_o and R-values for each extracted mixture binder. As indicated in Figure 4.7, the increase of the RAP content led to a resultant binder that was more aged than a control mixture with no RAP. However, the use of a softer binder or a WMA reversed the trend, showing that the softer binder helped in mitigating the aging of the binder that resulted from the RAP binder. Also, similar to the findings of the Black Space diagram, the results indicated that the softer binder had more effect in mitigating aging than the WMA technologies used.

19
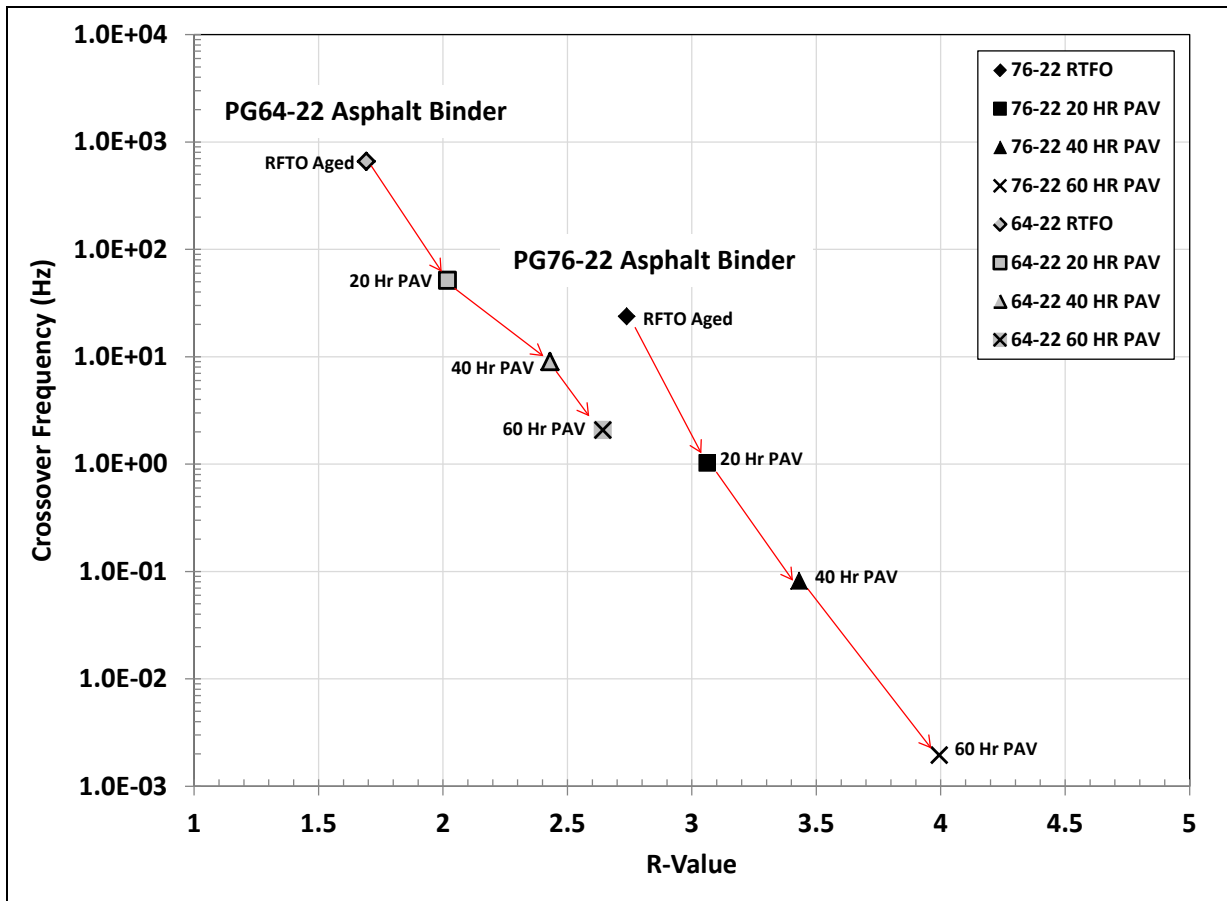
Figure 4.6: Crossover Frequency, R-value Space: PG64-22 and PG76-22 Asphalt Binders after Different Aging Levels
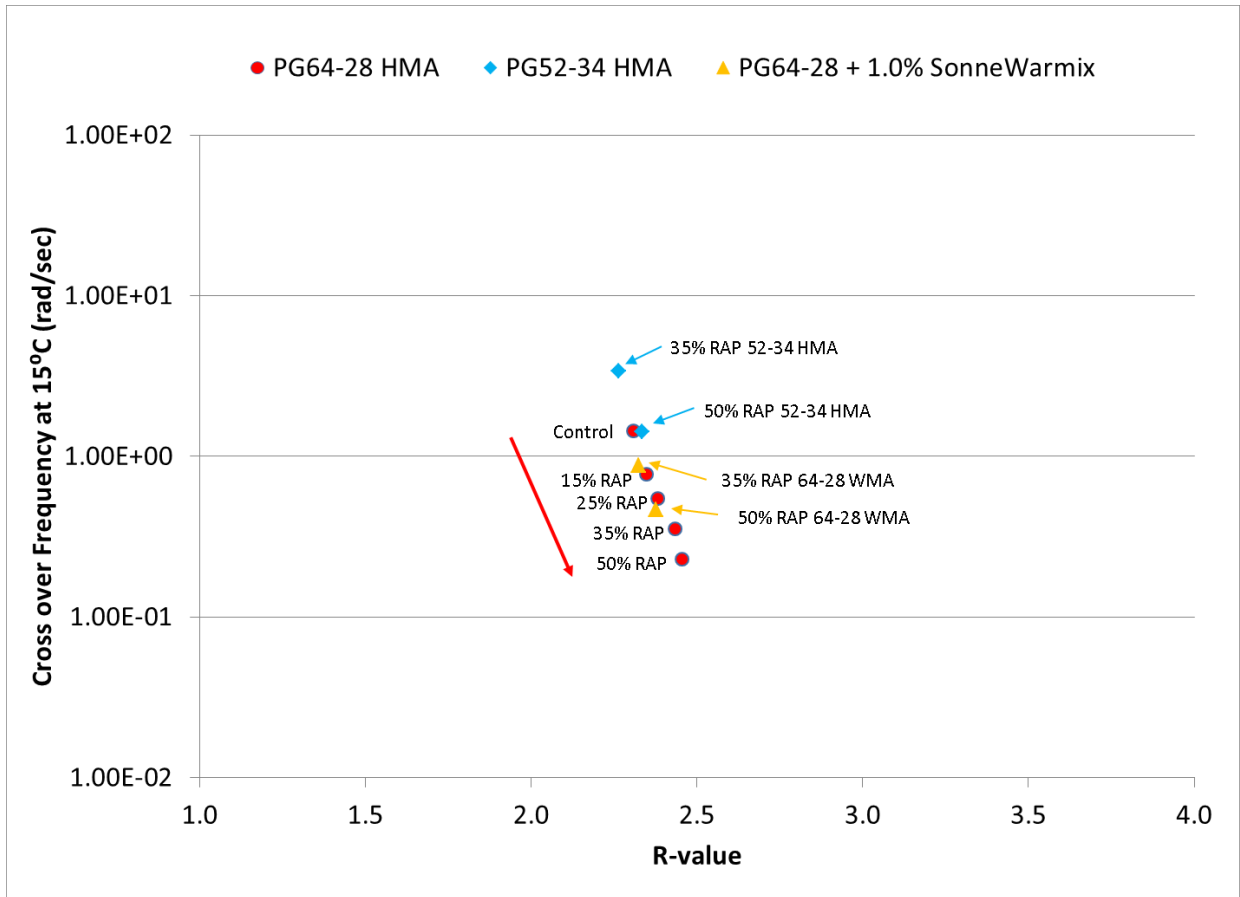
Figure 4.7: Crossover Frequency, R-value Space: Extracted Mixture Binders for This Study

Blank Page Inserted Intentionally

5.0 Mixtures Performance Tests and Results

This section outlines the mixture testing corresponding to the nine mixtures selected for evaluation, as shown previously in Table 3.3.

5.1 Rutting and Moisture Susceptibility,
Hamburg Wheel Tracking Device (HWTD)

Rutting and moisture damage was conducted in accordance with AASHTO T324 "Hamburg Wheel-Track Testing of Compacted Hot-Mix Asphalt (HMA)" (*2*). This test is used to determine the failure susceptibility of a mixture due to weakness in the aggregate structure, inadequate binder stiffness, or moisture damage (*2*). In this test, a mixture is submerged in heated water (typically 40º to 50ºC) and subjected to repeated loading provided by a 705N (158 lb.) steel wheel. As the steel wheel loads the specimen, the corresponding rut depth of the specimen is recorded. The rut depth versus the number of wheel passes is plotted in order to determine the Stripping Inflection Point (SIP), as shown in Figure 5.1. The SIP gives an indication of the point at which the test specimen begins to exhibit moisture damage (stripping).

Gyratory specimens for this test were fabricated using the Superpave gyratory compactor (SGC) to an air void level of 7.0±1.0%, as required by AASHTO T324. Testing was conducted at a temperature of 50ºC (122ºF). The specimens were tested at a rate of 52 passes per minute after a soak time of 30 minutes at the test temperature. Testing terminated at 20,000 wheel passes, or when visible stripping was noted. Figures 5.2 to 5.4 present the results of the Hamburg Wheel Tracking Device (HWTD).

The data in Figures 5.2 to 5.4 illustrate that the use of a softer binder with the 35% and 50% RAP led to an overall binder that was less stiff than binder resulting from the use of PG64-28 (i.e., increased rutting). This agreed with the Black Space and ω_o – R-value diagrams. Also, as illustrated in Figure 5.3, the two WMA technologies did not reduce the stiffness of the aging binder significantly, which again agreed with both binder testing diagrams.

Figure 5.1: Stripping Inflection Point

MassDOT RAP Study Hamburg Results
Laboratory Mixture

PG64-28 HMA - 0% RAP
Test Temperature: 45°C
Stripping Inflection Point: NONE
Rut Depth at 10,000: 0.60 mm
Rut Depth at 20,000: 1.40 mm

PG64-28 HMA - 15% RAP
Test Temperature: 45°C
Stripping Inflection Point: NONE
Rut Depth at 10,000: 0.41 mm
Rut Depth at 20,000: 0.61 mm

PG64-28 HMA - 25% RAP
Test Temperature: 45°C
Stripping Inflection Point: NONE
Rut Depth at 10,000: 1.02 mm
Rut Depth at 20,000: 1.39 mm

PG64-28 HMA - 35% RAP
Test Temperature: 45°C
Stripping Inflection Point: NONE
Rut Depth at 10,000: 0.32 mm
Rut Depth at 20,000: 0.40mm

PG64-28 HMA - 50% RAP
Test Temperature: 45°C
Stripping Inflection Point: NONE
Rut Depth at 10,000: 0.65 mm
Rut Depth at 20,000: 0.84 mm

MassDOT Criteria
1. A maximum rut depth of 12.5 mm at 20,000 passes for HMA and WMA.

2. No abrupt increase in the rate of deformation (Stripping Inflection Point) prior to 15,000 passes.

Legend:
PG64-28 HMA Control
PG64-28 HMA 15% RAP
PG64-28 HMA 25% RAP
PG64-28 HMA 35% RAP
PG64-28 HMA 50% RAP

Figure 5.2: HWTD Results for PG64-28 HMA Mixtures

25
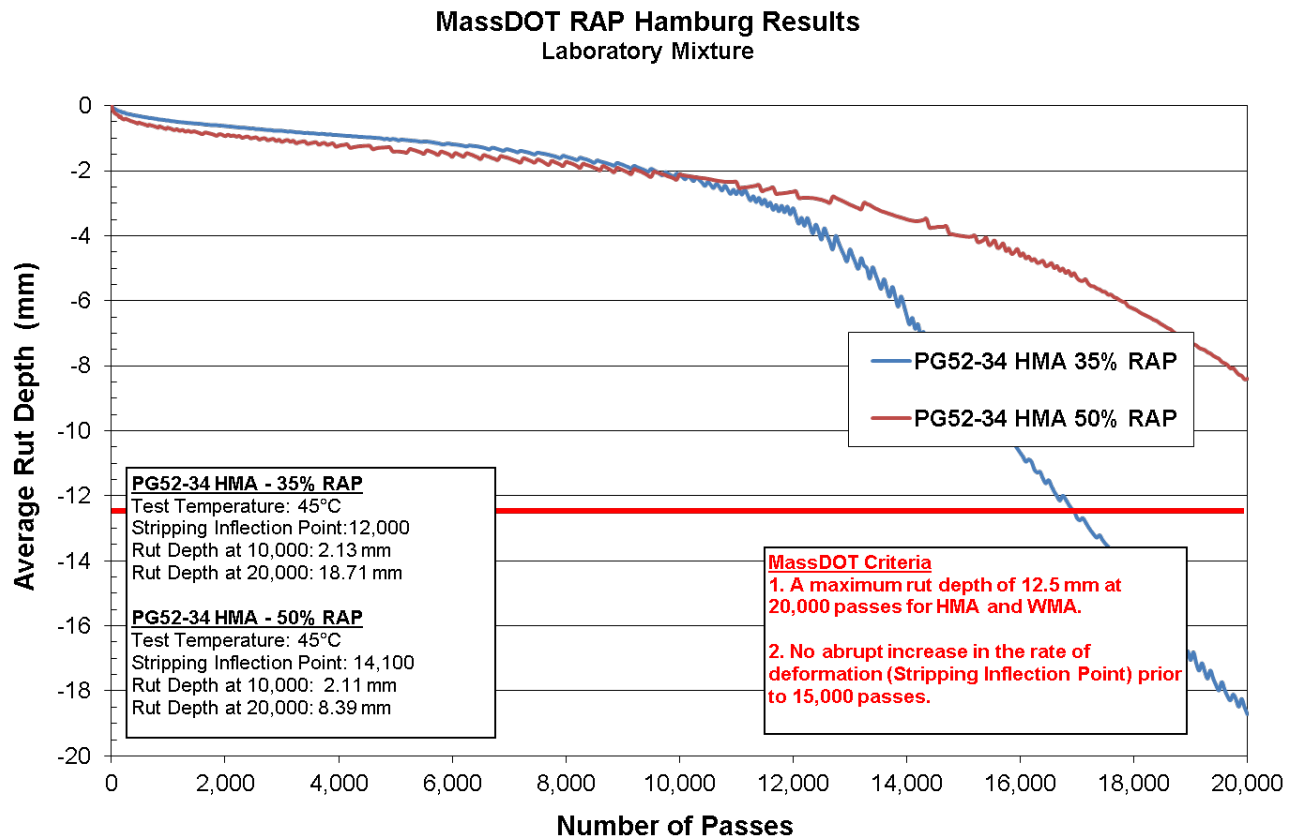
Figure 5.3: HWTD Results for PG52-34 HMA Mixtures

MassDOT RAP Hamburg Results
Laboratory Mixture

PG64-28 WMA - 35% RAP (1.0% SWM)
Test Temperature: 45°C
Stripping Inflection Point: NONE
Rut Depth at 10,000: 1.01 mm
Rut Depth at 20,000: 1.87 mm

PG64-28 WMA - 50% RAP (1.0% SWM)
Test Temperature: 45°C
Stripping Inflection Point: NONE
Rut Depth at 10,000: 1.26 mm
Rut Depth at 20,000: 1.79 mm

PG64-28 WMA - 35% RAP (0.5% Evotherm P15)
Test Temperature: 45°C
Stripping Inflection Point: NONE
Rut Depth at 10,000: 0.66 mm
Rut Depth at 20,000: 1.13 mm

PG64-28 WMA - 50% RAP (0.5% Evotherm P15)
Test Temperature: 45°C
Stripping Inflection Point: NONE
Rut Depth at 10,000: 1.17 mm
Rut Depth at 20,000: 1.68 mm

PG64-28 WMA 35% RAP (1.0% SWM)
PG64-28 WMA 50% RAP (1.0% SWM)
PG64-28 WMA 35% RAP (0.5% Evotherm P15)
PG64-28 WMA 50% RAP (0.5% Evotherm P15)

MassDOT Criteria
1. A maximum rut depth of 12.5 mm at 20,000 passes for HMA and WMA.

2. No abrupt increase in the rate of deformation (Stripping Inflection Point) prior to 15,000 passes.

Figure 5.4: HWTD Results for PG64-28 WMA Mixtures

5.2 Fatigue Cracking: Flexural Beam Fatigue

For this test, beam specimens were cut from slabs. Slabs with dimensions of 150 mm wide, 150 mm tall, and 450 mm long (6 in. wide, 6 in. tall, and 17.5 in. long) were fabricated for each mixture using the IPC Global Pressbox slab compactor. From each slab, beams with dimensions of 63 mm wide, 50 mm tall, and 380 mm long (2.5 in. wide, 2 in. tall, and 15 in. long) were cut such that the sides had smooth faces. The air voids of the final cut specimens were 7±1%.

Beam specimens were conditioned at the test temperature of 15°C (59ºF) for at least two hours prior to testing. Each beam fatigue test was conducted in strain control mode at a loading frequency of 10Hz applied using a sinusoidal waveform. Specimens were tested at a strain level of 500με because all mixtures lost 50% of their initial stiffness after at least 10,000 cycles. The number of cycles to mixture failure was determined by fitting an exponential function to the flexural stiffness versus number of cycles and then evaluating the

number of cycles that it took to decrease the initial stiffness by 50%. The beam fatigue testing results are shown in Figure 5.5.
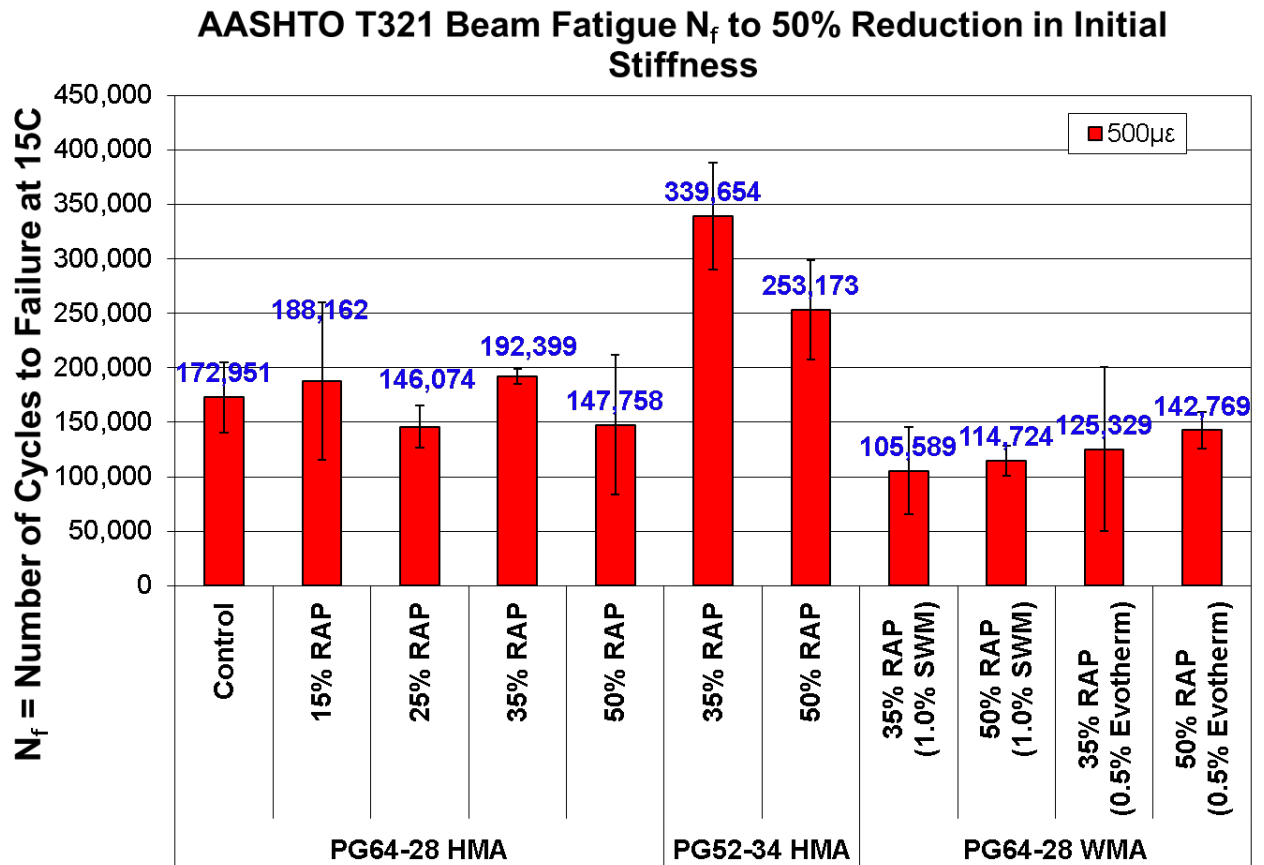
Figure 5.5: Beam Fatigue Results

The error bars shown in Figure 5.5 indicate the standard deviation of the cycle to failure measurements collected on multiple beams tested for each mixture. If the error bars overlapped between mixtures, the data was not significantly different. Generally, the PG64-28 HMA mixture at all RAP contents up to 50% RAP did not show a significant difference in fatigue cracking resistance. The use of the softer PG52-34 binder did show increased fatigue cracking resistance as compared to the PG64-28 HMA mixtures. This result agreed well with the Black Space and ω_o – R-value diagrams and the mixture rutting results, which likewise indicated that the mixture was less stiff (i.e., more crack resistant). The use of the WMA technology generally indicated reduced fatigue cracking resistance as compared to the other mixtures, but was generally only significant when compared to the PG52-34 mixtures.

Another component of this study was to investigate the effect of increased Voids in Mineral Aggregate (VMA) on the fatigue life of RAP mixtures. Increasing the VMA of the mixture would require redesigning the mixture with a different gradation and binder content, and thus would not be comparable to any mixtures in this study. In actuality, the concern with using higher percentages of RAP in the mixtures is whether or not all of the RAP binder can be

28

adequately utilized (i.e., 100% blending). If complete blending does not occur, then the mixture may have a lower effective asphalt binder content (under asphalted condition); this can then lead to performance degradation, particularly in terms of fatigue cracking. Thus, understanding the true contribution of the RAP binder to the overall mixture is of the utmost importance. In order to better understand this phenomenon, beam specimens were fabricated assuming only 70% of the RAP binder could be utilized for the 35% and 50% PG64-28 HMA mixtures. For these mixtures, the design binder content remained the same at 6.5%; however, the added virgin binder amount was increased compared to the previously tested mixtures, which assumed 100% contribution of the RAP binder. The beams were fabricated and prepared in the same manner previously described. For both the 35% and 50% RAP mixtures, as shown in Figure 5.6, assuming less contribution of RAP binder yields a mixture with more effective asphalt and thus the fatigue cracking resistance of the mixture is increased. Comparison of the volumetric data between the 100% and 70% contribution of RAP binder mixtures indicated very similar properties for the 35% RAP mixture, but less similar properties for the 50% RAP mixture. These results suggest the actual contribution of RAP binder may be not a fixed value, but rather varies based on RAP type and content.
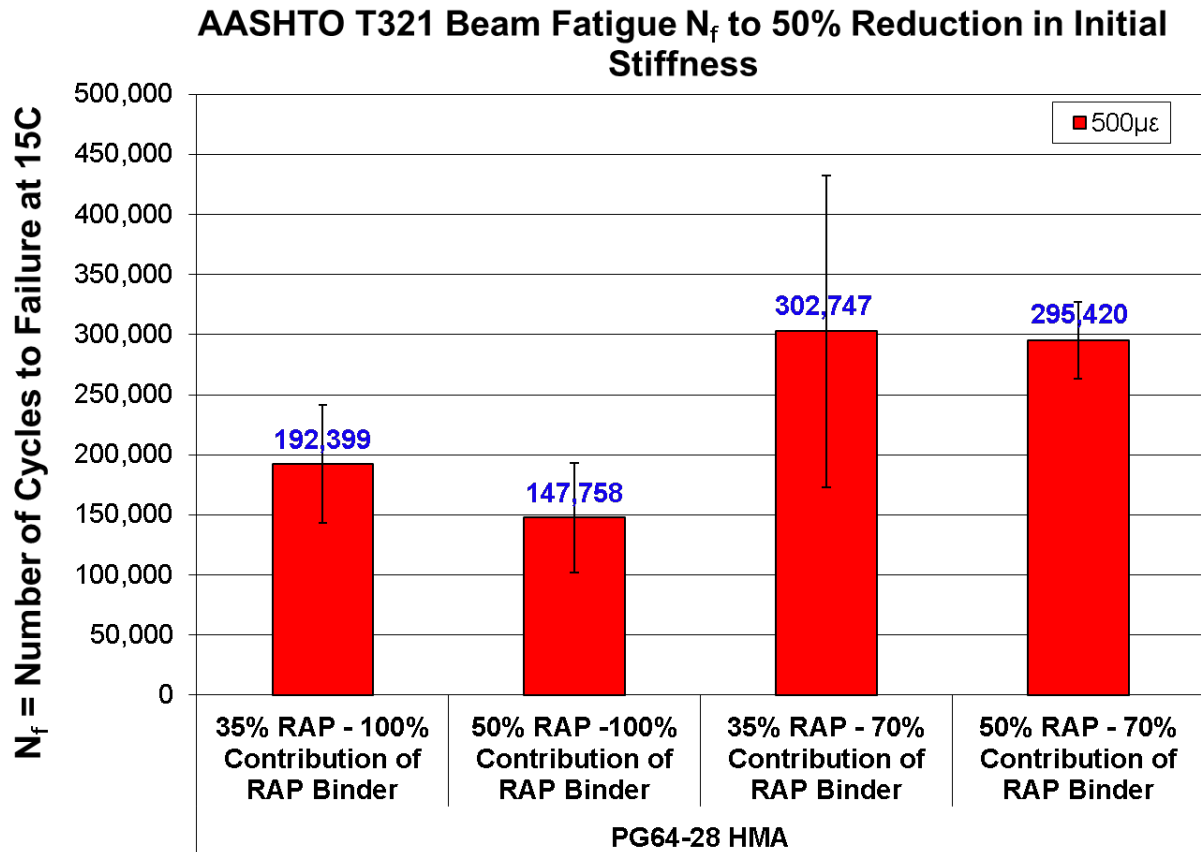
Figure 5.6: Beam Fatigue Results for Extra Added Binder

5.3 Workability: Asphalt Workability Device (AWD)

Because of the potential decrease in mixture workability due to the incorporation of higher amounts of RAP with and without WMA in the mixtures, workability evaluations of each of the mixtures were completed. These evaluations were conducted using an HMA workability device developed by the University of Massachusetts Dartmouth Highway Sustainability Research Center (HSRC). This device is known as the Asphalt Workability Device (AWD) and had been used previously to evaluate high percentage RAP mixtures as well as mixtures incorporating WMA additives (*12, 13*).

The AWD operates on the torque measurement principles that have been previously established (*14*). The AWD rotates the loose HMA mixture at a constant speed (15 rpm for this study) and separately records the resultant torque exerted on a pug mill style paddle shaft embedded into the mixture. The surface and internal temperatures of the mixture are recorded concurrently. As the mixture cools in ambient conditions, the torque exerted on the shaft increases, thereby giving an indication of the workability of the mixture at different temperatures. Each of the mixtures in this study was mixed and aged (four hours) at the mixing and compaction temperatures previously outlined. After completion of aging, the loose mixture was tested in the AWD.

From the AWD test data for each selected mixture, a best-fit exponential line was inserted into the raw data. This fit line was then used to develop a model curve plotted over the AWD test temperature range in which torque and temperature data were collected. This temperature range included the anticipated field placement and compaction temperatures of the mixture. The model curves are shown in Figure 5.7. Note that mixtures exhibiting lower torque values were considered more workable.
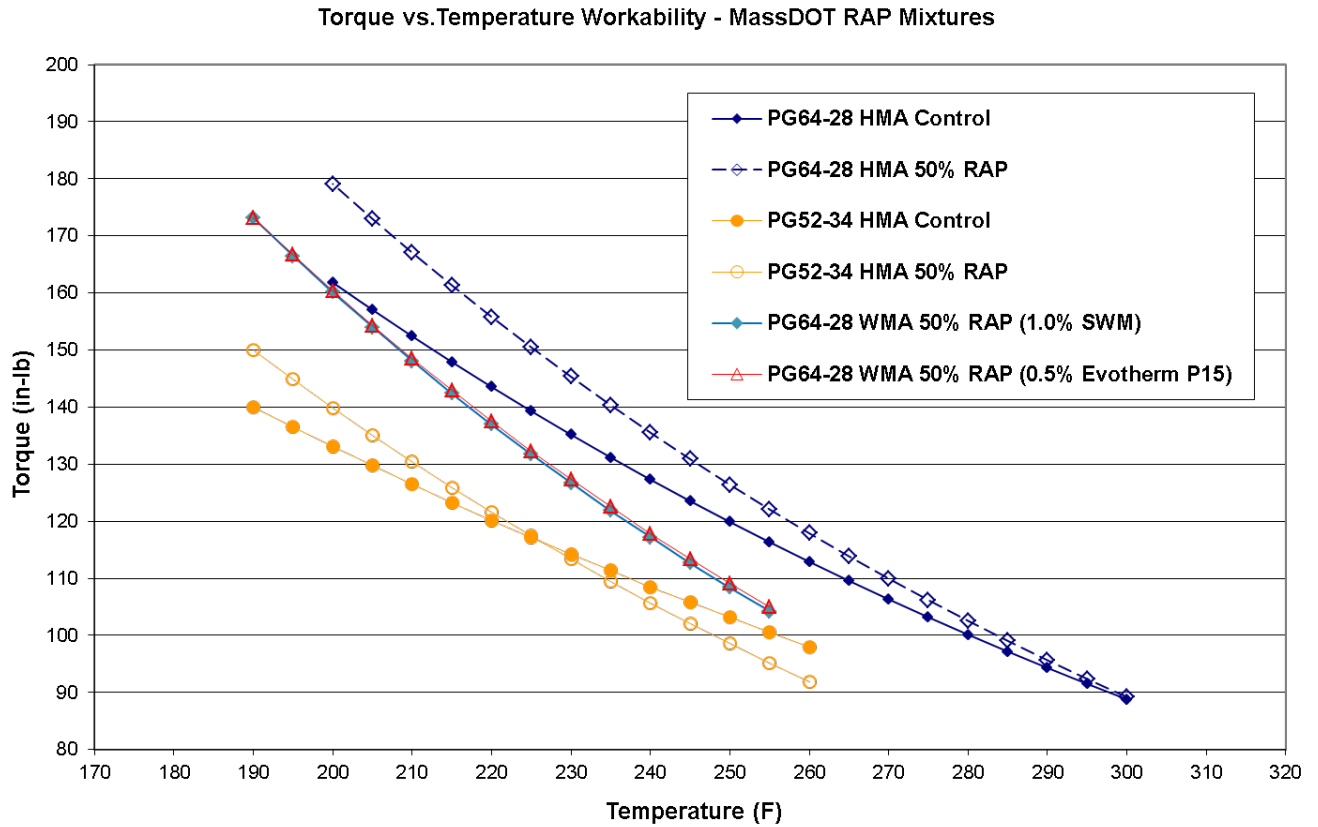
Figure 5.7: Mixture Workability Results

For the PG64-28 HMA mixtures, the workability data was consistent with the anticipated result and thus indicated that mixture workability is decreased as more RAP (50%) is introduced into the mixture, as compared to a mixture with no RAP (control). The use of the softer PG52-34 mixture showed increased mixture workability for both the control and 50% RAP mixtures compared to the PG64-28 HMA mixtures. This agreed well with the binder and mixture tests results that consistently indicated that the PG52-34 mixtures were less stiff than the other mixtures tested. The use of either WMA technology in the PG64-28 50% RAP mixture, at reduced mixing and compaction temperatures, indicated improved mixture workability over the corresponding 50% RAP HMA mixture and the control mixture. However, the improvement was not as great as exhibited by the softer binder (PG52-34) mixtures tested.

Overall, the workability data indicated that using increased amounts of RAP in the mixture will reduce mixture workability. Using a WMA technology or softer binder can improve these workability reductions, but their use must be balanced so that other performance indicators are not degraded.

Blank Page Inserted Intentionally

6.0 Chemical Analysis to Determine Quality and Degree of Blending of RAP Asphalt Binders Leading to Performance Prediction

Comprehensive testing of extracted and recovered binders from various mixtures was undertaken in order to understand the quality of asphalt blending in the various mixtures examined in this study. The quality of blending was determined by comparing the chemistries of the various blended asphalts to those of the PG64-28 control asphalt and the asphalt in the RAP stockpile. The specific details of this testing are located in a detailed report in Appendix 9.2.

6.1 Chemical Analysis Testing Conclusions and Recommendations

Asphalts are often classified as either a sol-type of asphalt (which has more compatible chemistries), or a gel-type of asphalt (which has less compatible chemistries). Asphalts with more compatible chemistries are usually more ductile, less elastic, more sensitive to temperature changes, and have low amounts of asphaltenes that are well dispersed or peptized by the maltene phase. Asphaltenes that allow themselves to be dispersed are called peptizable asphaltenes. Asphalts with less compatible chemistries usually have the opposite characteristics.

To determine the chemistries of the extracted and recovered asphalts, the asphaltene content of each asphalt was measured, along with a characterization of their state of dispersion in the maltene phase using the Heithaus compatibility parameters, p_a, p_o, and P. The parameter p_a measures the peptizability of the asphaltenes; p_o measures the solvent power of the maltenes; and P is a measure of the overall compatibility of the asphalt. Larger values of p_a, p_o, and P generally represent more peptizable asphaltenes, maltenes that are a good solvent, and an overall compatible asphalt. Smaller values of p_a, p_o, and P represent the reverse. It has been found that asphalts with high asphaltene contents generally have low p_a values, while some studies indicate that asphalts with high concentrations of polar aromatic materials should have high p_o values. It has also been generally found that p_a values will decrease while p_o values will increase with increasing oxidation of an asphalt. With aging, the asphaltenes become less peptizable, while the maltenes become a better solvent.

Evaluation of the compatibility parameters measured specifically for the 64-28 data sets suggests that the RAP Stockpile material is characterized by typical p-values for a mildly aged binder material, but the 64-28 control material (Base binder) is measured to have atypical p-values. Specifically, the low p_a value is more often characteristic of high asphaltene content, but in the present case asphaltene content is low. High p_o values are indicative of high concentrations of polar aromatic materials and/or a more complex chemical make (polymer or other type of modification) than is typical for a straight run

binder. It was further noted that the increase in asphaltene content for RAP blends was related to simulated mix conditioning at the plant; thus, it was observed that 64-28 WMA materials at the same RAP content showed less asphaltene content than 64-28 HMA materials. Based on the results presented, it is speculated that this particular blend of 64-28 control material with RAP is highly susceptible to oxidation conditions at the mixing plant. Blending theories of residua also suggest that blending materials with vastly different compatibility characteristics may result in very incompatible blends.

Additional testing may involve IR-spectrometric investigation to evaluate the extent of oxidation and to better characterize the starting and blended materials. Chromatographic separation (SARA, GPC, IEC) and material fraction physicochemical characterization (IR) of the 64-28 Control material may also provide additional information regarding this material's peculiar compatibility characteristics. Atomic force microscopic (AFM) studies may also provide further information regarding wax content, polymer modification, and the presence of recycled motor oil bottoms.

7.0 Conclusions

This study was conducted to better understand the impact of higher percentages of RAP in HMA mixtures. The following conclusions from the study should be verified for different mixtures and sources of RAP.

1. Superpave 9.5 mm mixtures were designed and incorporated varying RAP contents (15%, 25%, 35%, and 50% RAP) with the same binder content and gradation as the control mixture (0% RAP). At RAP contents beyond 50%, the gradation and binder content of the mixture could not be maintained to meet target volumetric properties.

2. PG64-28 and PG52-34 binders were used for this study. Confirmation of the AASHTO blending charts recommended the use of different asphalt binder grades. These grades are not typically specified in Massachusetts.

3. Binder data plotted on the Black Space diagram indicated for the PG64-28 HMA mixtures that the control mixtures and the RAP mixtures were in the onset of cracking zone. The mixtures edged closer to the failure zone, in terms of cracking due to aging, as the amount of RAP increased. The use of softer binder and WMA technologies assisted in reversing the trends for the 35% and the 50% RAP mixtures; however, both mixtures were still in the onset of cracking zone.

4. The binder ω_o and R-value plot indicated, for the PG64-28 HMA mixture, that the use of more RAP led to a resultant binder that is more aged than a control mixture with no RAP. The use of a softer binder or a WMA technology reversed the trend. Similar to the results of the Black Space diagram, the ω_o and R-value plot indicated that the softer binder had more effect in mitigating the aging of the resultant binder than the WMA technologies used.

5. The HWTD data illustrated that the use of a softer binder with the 35% and 50% RAP led to an overall binder that was less stiff than when the PG64-28 binder was used (i.e., increased rutting). This agreed with the Black-Space and ω_o – R-value diagrams. Also, the two WMA technologies did not reduce the stiffness of the aging binder significantly, which again agreed with both binder testing diagrams.

6. The PG64-28 HMA mixture at all RAP contents up to 50% RAP did not show a significant difference in fatigue cracking resistance. The use of the softer PG52-34 binder did show increased fatigue cracking resistance compared to the PG64-28 HMA mixtures. This result agreed well with the Black Space and ω_o – R-value diagrams and the mixture rutting results, both of which indicated that the mixture was less stiff (i.e., more crack resistant). The use of the WMA technology generally indicated reduced fatigue cracking resistance compared to the other mixtures, but was generally only significant when compared to the PG52-34 mixtures.

7. Analysis of a reduced contribution of binder from the RAP suggested that the actual contribution of RAP binder may not be a fixed value; rather, it varies based on RAP type and content.

8. The workability data indicated that using increased amounts of RAP in the mixture will reduce mixture workability. Using a WMA technology or a softer binder can improve these workability reductions, but their use must be balanced so that other performance indicators are not degraded.

9. Using a softer binder or a WMA technology alone did not yield a mixture with the same performance as an all-virgin material mixture. Thus, the use of higher percentages of RAP in HMA must be carefully developed for each specific mixture based on the properties of the RAP, the amount of RAP, available virgin binders, and available WMA technologies.

10. The use of asphalt rejuvenators should be investigated for these types of mixtures in an effort to reuse more of the binder in the RAP.

8.0 References

1. Newcomb, D. and C. Jones. The State of HMA Recycling in the U.S. *Hot Mix Asphalt Technology*, July/August 2008, pp. 20–25.

2. *Standard Specifications for Transportation Materials and Methods of Sampling and Testing, 30th Ed*. American Association of State Highway and Transportation Officials, Washington, D.C., 2010.

3. McDaniel, R. and R. M. Anderson. *Recommended Use of Reclaimed Asphalt Pavement in the Superpave Mix Design Method: Technician's Manual*. Report 452. National Cooperative Highway Research Program, 2001.

4. Engstrom, B. Optimizing the Use of Recycled Asphalt Pavement in Thin Lift HMA Mixtures Using Warm Mix Asphalt Technology. Master's Thesis. University of Massachusetts, Dartmouth, Sept. 2008.

5. Mogawer, W. S., A. Booshehrian, S. Vahidi, and A. J. Austerman. Evaluating the Effect of Rejuvenators on the Degree of Blending and Performance of High RAP, RAS, RAP/RAS Mixtures. *Journal of the Association of Asphalt Paving Technologist*, Vol. 82, 2013, pp. 403–436.

6. King, G., M. Anderson, D. Hanson, and P. Blankenship. Using Black Space Diagrams to Predict Age-Induced Cracking. 7th RILEM International Conference on Cracking in Pavements. *RILEM Book Series*, Vol. 4, 2012, pp. 453–463.

7. Anderson, M., G. King, D. Hanson, and P. Blankenship. Evaluation of the Relationship between Asphalt Binder Properties and Non-Load Related Cracking. *Journal of the Association of Asphalt Paving Technologist*, Vol. 80, 2011, pp. 615–661.

8. Glover, C. J., R. R. Davison, C. H. Domke, Y. Ruan, P. Juristyarini, D. B. Knorr, and S. H. Jung. *Development of a New Method for Assessing Asphalt Binder Durability with Field Evaluation*. Report FHWA/TX-05/1872-2. Federal Highway Administration and Texas Department of Transportation, Aug. 2005.

9. Rowe, G. Analysis of SHRP Core Asphalts—New 2013/14 Test Results. Presented at Binder Expert Task Group Meeting, San Antonio, TX, 2014.

10. Daniel, J. S. AAPT Symposium: Recycling with RAP, RAS, and Secondary Aggregates. *Journal of the Association of Asphalt Paving Technologist*, Vol. 82, 2013, pp. 661–682.

11. Christensen, D., and D. Anderson. Interpretation of Dynamic Mechanical Test Data for Paving Grade Asphalt. *Journal of the Association of Asphalt Paving Technologists*, Vol. 61, 1992, pp. 67–116.

12. Austerman, A. J., W. S. Mogawer, and R. Bonaquist. Investigation of the Influence of Warm Mix Asphalt Additive Dose on the Workability, Cracking Susceptibility, and Moisture Susceptibility of Asphalt Mixtures Containing Reclaimed Asphalt Pavement. In *Canadian Technical Asphalt Association Proceedings*, Moncton, New Brunswick, Nov. 2009, pp. 51–71.

13. Mogawer, W. S., A. J. Austerman, and M. Roussel. Performance Characteristics of Asphalt Rubber Mixtures Containing RAP and Warm Mix Asphalt Technology. In *Proceedings of the 2nd International Warm-Mix Conference*, St. Louis, MO, Oct. 2011.

14. Gudimettla, J., L. Cooley, and E. Brown. *Workability of Hot Mix Asphalt*. Report #03-03. National Center for Asphalt Technology, Auburn, AL, 2003.

9.0 Appendices

Appendix 9.1 Mixture Design Data

PG64-28 HMA						
Mixture	**Control REDO**	**15% RAP HMA**	**25% RAP HMA**	**35% RAP HMA**	**50% RAP HMA**	**75% RAP HMA**
Binder Type	PG64-28	PG64-28	PG64-28	PG64-28	PG64-28	PG64-28
Percent Binder, Total Mix	6.50%	6.50%	6.50%	6.50%	6.50%	6.50%
WMA Type	NONE	NONE	NONE	NONE	NONE	NONE
WMA Dose	-	-	-	-	-	-
Mixing Temp.	324-315	324-316	324-316	324-317	324-316	324-316
Compaction Temp.	306-294	306-295	306-295	306-296	306-295	306-295
Aging Time at Compaction Temp.	2 hrs.	2 hrs.	2 hrs.	2 hrs.	2 hrs.	2 hrs.
RAP Time on Heated Aggregates	n/a	2 hrs.	2 hrs.	2 hrs.	2 hrs.	2 hrs.
Specimen Height #1, mm	118.2	119.0	118.5	119.0	118.0	117.6
Specimen Height #2, mm	118.3	118.0	118.2	118.5	118.3	117.1
Specimen Height #3, mm	118.6	118.6	118.0	118.1	117.9	118.0
Average Specimen Height, mm	*118.4*	*118.5*	*118.2*	*118.5*	*118.1*	*117.6*
Bulk Specific Gravity, Spec. #1 Gmb	2.314	2.292	2.300	2.294	2.310	2.320
Bulk Specific Gravity, Spec. #2 Gmb	2.316	2.311	2.313	2.305	2.306	2.324
Bulk Specific Gravity, Spec. #3 Gmb	2.304	2.301	2.309	2.315	2.306	2.315
Bulk Specific Gravity, Avg. Gmb	*2.311*	*2.301*	*2.307*	*2.305*	*2.307*	*2.320*
Max. Theo. Specific Gravity, Spec. #1 Gmm		2.412	2.417	2.416	2.422	2.418
Max. Theo. Specific Gravity, Spec. #2 Gmm		2.418	2.413	2.417	2.420	2.419
Max. Theo. Specific Gravity, Avg. Gmm	*2.405*	*2.415*	*2.415*	*2.417*	*2.421*	*2.419*
Air Voids -Spec. #1, %	3.78		4.76	5.09	4.58	4.09
Air Voids -Spec. #2, %	3.7	4.31	4.22	4.63	4.75	3.93
Air Voids -Spec. #3, %	4.2	4.72	4.39	4.22	4.75	4.3
Average Air Voids, %	*3.89*	*4.52*	*4.46*	*4.65*	*4.69*	*4.11*
VMA -Spec. #1, %	15		15.5	15.7	15.1	14.7
VMA -Spec. #3, %	14.9	15.1	15.0	15.3	15.2	14.6
VMA -Spec. #2, %	15.3	15.4	15.1	14.9	15.2	14.9
Average VMA, %	*15.1*	*15.3*	*15.2*	*15.3*	*15.2*	*14.7*
VFA -Spec. #1, %	74.8		69.3	67.6	69.7	72.2
VFA -Spec. #2, %	75.2	71.5	71.9	69.7	68.8	73.1
VFA -Spec. #3, %	72.5	69.4	70.9	71.7	68.8	71.1
Average VFA, %	*74.2*	*70.5*	*70.7*	*69.7*	*69.1*	*72.1*
Effective Aggregate Specific Gravity, Gse	*2.665*	*2.678*	*2.678*	*2.681*	*2.686*	*2.684*
Percent Binder Absorbed, %	*1.78*	*1.97*	*1.97*	*2.01*	*2.08*	*2.05*
Percent Binder Effective, Pbe %	*4.84*	*4.66*	*4.66*	*4.62*	*4.56*	*4.58*
Dust to Binder Ratio	*1.24*	*1.29*	*1.29*	*1.3*	*1.32*	*1.31*

Mixture	Control REDO	15% RAP WMA	25% RAP WMA REDO	35% RAP WMA	50% RAP WMA
PG64-28 WMA 1.0% SonneWarmix (By Total Binder Weight).					
Binder Type	PG64-28	PG64-28	PG64-28	PG64-28	PG64-28
Percent Binder, Total Mix	6.50%	6.50%	6.50%	6.50%	6.50%
WMA Type	SonneWarmix	SonneWarmix	SonneWarmix	SonneWarmix	SonneWarmix
WMA Dose	1.00%	1.00%	1.00%	1.00%	1.00%
Mixing Temp.	275	275	275	275	275
Compaction Temp.	256	256	256	256	256
Aging Time at Compaction Temp.	2 hrs.	2 hrs.	2 hrs.	2 hrs.	2 hrs.
RAP Time on Heated Aggregates	n/a	2 hrs.	2 hrs.	2 hrs.	2 hrs.
Specimen Height #1, mm	118.2	118.9	118.6	118.4	118.8
Specimen Height #2, mm	118.5	119.6	118.6	118.7	117.8
Specimen Height #3, mm	117.6	118.3	118.3	118.1	119.0
Average Specimen Height, mm	***118.1***	***118.9***	***118.5***	***118.4***	***118.5***
Bulk Specific Gravity, Spec. #1 Gmb	2.312	2.292	2.303	2.304	2.295
Bulk Specific Gravity, Spec. #2 Gmb	2.311	2.309	2.306	2.291	2.316
Bulk Specific Gravity, Spec. #3 Gmb	2.326	2.305	2.308	2.311	2.292
Bulk Specific Gravity, Avg. Gmb	***2.316***	***2.302***	***2.306***	***2.302***	***2.301***
Max. Theo. Specific Gravity, Spec. #1 Gmm		2.407		2.410	2.416
Max. Theo. Specific Gravity, Spec. #2 Gmm		2.404			2.416
Max. Theo. Specific Gravity, Avg. Gmm	***2.404***	***2.406***	***2.403***	***2.410***	***2.416***
Air Voids -Spec. #1, %	3.83	4.74	4.16	4.40	5.01
Air Voids -Spec. #2, %	3.87	4.03	4.04	4.94	4.14
Air Voids -Spec. #3, %	3.24	4.20	3.95	4.11	5.13
Average Air Voids, %	***3.65***	***4.32***	***4.05***	***4.48***	***4.76***
VMA -Spec. #1, %	15.0	15.8	15.4	15.3	15.7
VMA -Spec. #3, %	15.1	15.1	15.2	15.8	14.9
VMA -Spec. #2, %	14.5	15.3	15.2	15.1	15.8
Average VMA, %	***14.9***	***15.4***	***15.3***	***15.4***	***15.5***
VFA -Spec. #1, %	74.5	70.0	73.0	71.2	68.1
VFA -Spec. #2, %	74.4	73.3	73.4	68.7	72.2
VFA -Spec. #3, %	77.7	72.5	74.0	72.8	67.5
Average VFA, %	***75.5***	***71.9***	***73.5***	***70.9***	***69.3***
Effective Aggregate Specific Gravity, Gse	***2.664***	***2.667***	***2.663***	***2.672***	***2.68***
Percent Binder Absorbed, %	***1.77***	***1.81***	***1.76***	***1.88***	***1.99***
Percent Binder Effective, Pbe %	***4.85***	***4.81***	***4.85***	***4.74***	***4.64***
Dust to Binder Ratio	***1.24***	***1.25***	***1.24***	***1.27***	***1.29***

Mixture	Control EVO	15% RAP WMA EVO	25% RAP WMA EVO	35% RAP WMA EVO	50% RAP WMA EVO
PG64-28 WMA 0.5% Evotherm P15 (By Total Binder Weight).					
Binder Type	PG64-28	PG64-28	PG64-28	PG64-28	PG64-28
Percent Binder, Total Mix	6.50%	6.50%	6.50%	6.50%	6.50%
WMA Type	Evotherm	Evotherm	Evotherm	Evotherm	Evotherm
WMA Dose	0.50%	0.50%	0.50%	0.50%	0.50%
Mixing Temp.	275	275	275	275	275
Compaction Temp.	256	256	256	256	256
Aging Time at Compaction Temp.	2 hrs.	2 hrs.	2 hrs.	2 hrs.	2 hrs.
RAP Time on Heated Aggregates	n/a	2 hrs.	2 hrs.	2 hrs.	2 hrs.
Specimen Height #1, mm	118.4	118.6	119.0	118.9	119.5
Specimen Height #2, mm	118.3	118.5	119.0	119.5	119.0
Specimen Height #3, mm	118.6	119.1	119.2	119.4	118.6
Average Specimen Height, mm	***118.4***	***118.7***	***119.1***	***119.3***	***119.0***
Bulk Specific Gravity, Spec. #1 Gmb	2.305	2.303	2.295	2.294	2.285
Bulk Specific Gravity, Spec. #2 Gmb	2.306	2.301	2.293	2.284	2.296
Bulk Specific Gravity, Spec. #3 Gmb	2.302	2.293	2.292	2.286	2.309
Bulk Specific Gravity, Avg. Gmb	***2.304***	***2.299***	***2.293***	***2.288***	***2.297***
Max. Theo. Specific Gravity, Spec. #1 Gmm	2.403	2.410	2.414	2.416	2.427
Max. Theo. Specific Gravity, Spec. #2 Gmm	2.407	2.409	2.411	2.414	2.425
Max. Theo. Specific Gravity, Avg. Gmm	***2.405***	***2.410***	***2.413***	***2.415***	***2.426***
Air Voids -Spec. #1, %	4.16	4.44	4.89	5.01	5.81
Air Voids -Spec. #2, %	4.12	4.52	4.97	5.42	5.36
Air Voids -Spec. #3, %	4.28	4.85	5.01	5.34	4.82
Average Air Voids, %	***4.19***	***4.60***	***4.96***	***5.26***	***5.33***
VMA -Spec. #1, %	15.3	15.4	15.7	15.7	16.0
VMA -Spec. #3, %	15.2	15.4	15.7	16.1	15.6
VMA -Spec. #2, %	15.4	15.7	15.8	16.0	15.1
Average VMA, %	***15.3***	***15.5***	***15.7***	***15.9***	***15.6***
VFA -Spec. #1, %	72.8	71.2	68.9	68.1	63.7
VFA -Spec. #2, %	72.9	70.6	68.3	66.3	65.6
VFA -Spec. #3, %	72.2	69.1	68.3	66.6	68.1
Average VFA, %	***72.6***	***70.3***	***68.5***	***67.0***	***65.8***
Effective Aggregate Specific Gravity, Gse	***2.665***	***2.672***	***2.676***	***2.678***	***2.693***
Percent Binder Absorbed, %	***1.78***	***1.88***	***1.94***	***1.97***	***2.17***
Percent Binder Effective, Pbe %	***4.84***	***4.74***	***4.69***	***4.66***	***4.47***
Dust to Binder Ratio	***1.24***	***1.27***	***1.28***	***1.29***	***1.34***

PG52-34 HMA						
Mixture	**Control**	**15% RAP HMA**	**25% RAP HMA**	**35% RAP HMA**	**50% RAP HMA REDO**	**75% RAP HMA**
Binder Type	PG52-34	PG52-34	PG52-34	PG52-34	PG52-34	PG52-34
Percent Binder, Total Mix	6.50%	6.50%	6.50%	6.50%	6.50%	6.50%
WMA Type	NONE	NONE	NONE	NONE	NONE	NONE
WMA Dose	-	-	-	-	-	-
Mixing Temp.	296-283	296-283	296-283	296-283	296-283	296-283
Compaction Temp.	260-239	260-239	260-239	260-239	260-239	260-239
Aging Time at Compaction Temp.	2 hrs.	2 hrs.	2 hrs.	2 hrs.	2 hrs.	2 hrs.
RAP Time on Heated Aggregates	n/a	2 hrs.	2 hrs.	2 hrs.	2 hrs.	2 hrs.
Specimen Height #1, mm	118.5	118.7	118.5	118.6	118.7	118.9
Specimen Height #2, mm	118.1	118.8	118.1	118.4	118.5	118.8
Specimen Height #3, mm	118.5		118.8	118.7	119.2	118.5
Average Specimen Height, mm	*118.4*	*118.8*	*118.5*	*118.6*	*118.8*	*118.7*
Bulk Specific Gravity, Spec. #1 Gmb	2.301	2.300	2.301	2.300	2.298	2.294
Bulk Specific Gravity, Spec. #2 Gmb	2.308	2.302	2.306	2.306	2.305	2.294
Bulk Specific Gravity, Spec. #3 Gmb	2.306		2.303	2.303	2.290	2.304
Bulk Specific Gravity, Avg. Gmb	*2.305*	*2.301*	*2.303*	*2.303*	*2.298*	*2.297*
Max. Theo. Specific Gravity, Spec. #1 Gmm	2.401	2.406	2.409	2.417		2.414
Max. Theo. Specific Gravity, Spec. #2 Gmm	2.399	2.406	2.409	2.415		2.414
Max. Theo. Specific Gravity, Avg. Gmm	*2.400*	*2.406*	*2.409*	*2.416*	*2.413*	*2.414*
Air Voids -Spec. #1, %	4.12	4.41	4.48	4.80	4.77	4.97
Air Voids -Spec. #2, %	3.83	4.32	4.28	4.55	4.48	4.97
Air Voids -Spec. #3, %	3.92		4.40	4.68	5.10	4.56
Average Air Voids, %	*3.96*	*4.37*	*4.39*	*4.68*	*4.78*	*4.83*
VMA -Spec. #1, %	15.4	15.5	15.4	15.5	15.5	15.7
VMA -Spec. #3, %	15.2	15.4	15.2	15.2	15.3	15.7
VMA -Spec. #2, %	15.2		15.4	15.4	15.8	15.3
Average VMA, %	*15.3*	*15.5*	*15.3*	*15.4*	*15.5*	*15.6*
VFA -Spec. #1, %	73.2	71.5	70.9	69	69.2	68.3
VFA -Spec. #2, %	74.8	71.9	71.8	70.1	70.7	68.3
VFA -Spec. #3, %	74.2		71.4	69.6	67.7	70.2
Average VFA, %	*74.1*	*71.7*	*71.4*	*69.6*	*69.2*	*68.9*
Effective Aggregate Specific Gravity, Gse	*2.659*	*2.667*	*2.671*	*2.68*	*2.676*	*2.677*
Percent Binder Absorbed, %	*1.70*	*1.81*	*1.87*	*1.99*	*1.94*	*1.95*
Percent Binder Effective, Pbe %	*4.91*	*4.81*	*4.75*	*4.64*	*4.69*	*4.68*
Dust to Binder Ratio	*1.22*	*1.25*	*1.26*	*1.29*	*1.28*	*1.28*

PG52-34 WMA 1.0% SonneWarmix (By Total Binder Weight).

Mixture	Control	15% RAP WMA REDO	25% RAP WMA	35% RAP WMA	50% RAP WMA REDO
Binder Type	PG52-34	PG52-34	PG52-34	PG52-34	PG52-34
Percent Binder, Total Mix	6.50%	6.50%	6.50%	6.50%	6.50%
WMA Type	SonneWarmix	SonneWarmix	SonneWarmix	SonneWarmix	SonneWarmix
WMA Dose	1.00%	1.00%	1.00%	1.00%	1.00%
Mixing Temp.	245	245	245	245	245
Compaction Temp.	220	220	220	220	220
Aging Time at Compaction Temp.	2 hrs.	2 hrs.	2 hrs.	2 hrs.	2 hrs.
RAP Time on Heated Aggregates	n/a	2 hrs.	2 hrs.	2 hrs.	2 hrs.
Specimen Height #1, mm	118.1	118.7	118.6	116.6	118.5
Specimen Height #2, mm	118.3	118.7	118.7	118.3	118.7
Specimen Height #3, mm	118.2	118.7	118.6	118.6	119.1
Average Specimen Height, mm	*118.2*	*118.7*	*118.6*	*117.8*	*118.8*
Bulk Specific Gravity, Spec. #1 Gmb	2.309	2.298	2.303	2.343	2.304
Bulk Specific Gravity, Spec. #2 Gmb	2.311	2.298	2.299	2.311	2.300
Bulk Specific Gravity, Spec. #3 Gmb	2.312	2.309	2.303	2.308	2.294
Bulk Specific Gravity, Avg. Gmb	*2.311*	*2.302*	*2.302*	*2.321*	*2.299*
Max. Theo. Specific Gravity, Spec. #1 Gmm	2.396		2.404	2.409	
Max. Theo. Specific Gravity, Spec. #2 Gmm	2.394		2.404	2.406	
Max. Theo. Specific Gravity, Avg. Gmm	*2.395*	*2.399*	*2.404*	*2.408*	*2.413*
Air Voids -Spec. #1, %	3.59	4.21	4.20		4.52
Air Voids -Spec. #2, %	3.51	4.21	4.37	4.03	4.68
Air Voids -Spec. #3, %	3.47	3.75	4.20	4.15	4.93
Average Air Voids, %	*3.52*	*4.06*	*4.26*	*4.09*	*4.71*
VMA -Spec. #1, %	15.1	15.5	15.4		15.3
VMA -Spec. #3, %	15.1	15.5	15.5	15.1	15.5
VMA -Spec. #2, %	15.0	15.1	15.4	15.2	15.7
Average VMA, %	*15.1*	*15.4*	*15.4*	*15.2*	*15.5*
VFA -Spec. #1, %	76.2	72.8	72.7		70.5
VFA -Spec. #2, %	76.8	72.8	71.8	73.3	69.8
VFA -Spec. #3, %	76.9	75.2	72.7	72.7	68.6
Average VFA, %	*76.6*	*73.6*	*72.4*	*73.0*	*69.6*
Effective Aggregate Specific Gravity, Gse	*2.652*	*2.657*	*2.664*	*2.669*	*2.676*
Percent Binder Absorbed, %	*1.60*	*1.67*	*1.77*	*1.84*	*1.94*
Percent Binder Effective, Pbe %	*5.00*	*4.94*	*4.85*	*4.78*	*4.69*
Dust to Binder Ratio	*1.2*	*1.21*	*1.24*	*1.26*	*1.28*

Mixture	Control EVO	15% RAP WMA EVO	25% RAP WMA EVO	35% RAP WMA EVO	50% RAP WMA EVO
PG52-34 WMA 0.5% Evotherm P15 (By Total Binder Weight).					
Binder Type	PG64-28	PG64-28	PG64-28	PG64-28	PG64-28
Percent Binder, Total Mix	6.50%	6.50%	6.50%	6.50%	6.50%
WMA Type	Evotherm	Evotherm	Evotherm	Evotherm	Evotherm
WMA Dose	0.50%	0.50%	0.50%	0.50%	0.50%
Mixing Temp.	245	245	245	245	245
Compaction Temp.	220	220	220	220	220
Aging Time at Compaction Temp.	2 hrs.	2 hrs.	2 hrs.	2 hrs.	2 hrs.
RAP Time on Heated Aggregates	n/a	2 hrs.	2 hrs.	2 hrs.	2 hrs.
Specimen Height #1, mm	118.5	118.4	118.8	119.1	119.0
Specimen Height #2, mm	118	118.4	119.2	119.4	119.1
Specimen Height #3, mm	118.3	118.4	118.9	119.3	119.5
Average Specimen Height, mm	*118.3*	*118.4*	*119.0*	*119.3*	*119.2*
Bulk Specific Gravity, Spec. #1 Gmb	2.308	2.305	2.296	2.291	2.298
Bulk Specific Gravity, Spec. #2 Gmb	2.314	2.306	2.287	2.283	2.295
Bulk Specific Gravity, Spec. #3 Gmb	2.309	2.306	2.297	2.288	2.286
Bulk Specific Gravity, Avg. Gmb	*2.310*	*2.306*	*2.293*	*2.287*	*2.293*
Max. Theo. Specific Gravity, Spec. #1 Gmm	2.396	2.407	2.409	2.408	2.413
Max. Theo. Specific Gravity, Spec. #2 Gmm	2.396	2.405	2.409	2.401	2.412
Max. Theo. Specific Gravity, Avg. Gmm	*2.396*	*2.406*	*2.409*	*2.405*	*2.413*
Air Voids -Spec. #1, %	3.67	4.20	4.69	4.74	4.77
Air Voids -Spec. #2, %	3.42	4.16	5.06	5.07	4.89
Air Voids -Spec. #3, %	3.63	4.16	4.65	4.86	5.26
Average Air Voids, %	*3.57*	*4.17*	*4.80*	*4.89*	*4.97*
VMA -Spec. #1, %	15.2	15.3	15.6	15.8	15.5
VMA -Spec. #3, %	15.0	15.2	15.9	16.1	15.7
VMA -Spec. #2, %	15.1	15.2	15.6	15.9	16.0
Average VMA, %	*15.1*	*15.2*	*15.7*	*15.9*	*15.7*
VFA -Spec. #1, %	75.9	72.5	69.9	70.0	69.2
VFA -Spec. #2, %	77.2	72.6	68.2	68.5	68.9
VFA -Spec. #3, %	76.0	72.6	70.2	69.4	67.1
Average VFA, %	*76.4*	*72.6*	*69.4*	*69.3*	*68.4*
Effective Aggregate Specific Gravity, Gse	*2.654*	*2.667*	*2.671*	*2.665*	*2.676*
Percent Binder Absorbed, %	*1.63*	*1.81*	*1.87*	*1.78*	*1.94*
Percent Binder Effective, Pbe %	*4.98*	*4.81*	*4.75*	*4.84*	*4.69*
Dust to Binder Ratio	*1.2*	*1.25*	*1.26*	*1.24*	*1.28*

Appendix 9.2 Report: "Chemical Evaluation of RAP Asphalt Binders Leading to Performance Prediction"

Western Research
INSTITUTE

UMASS Project:

Chemical Evaluation of RAP Asphalt Binders Leading to Performance Prediction

Final Report

April 2015

Prepared for
Walaa Mogawer
UMASS-Dartmouth

Prepared by
WRI Transportation Technology Group
Troy Pauli, Principal Scientist
Steve Salmans, Senior Scientist
Jean-Pascal Planche, Vice-President

www.westernresearch.org

INTRODUCTION

Current Practice of RAP Neat Binder Property Characterization

To account for and offset binder stiffening effects and to improve mixture resistance to cracking with addition of RAP to asphalt pavement mixtures, two approaches have been taken. The first approach relies on blending charts to select softer virgin binders in high RAP mixtures. This approach was evaluated in NCHRP Project 9-12 [McDaniel et al. 2000] and is currently used in AASHTO M 323, *Standard Specification for Superpave Volumetric Mix Design*. The second approach relies on recycling agents (RA) to soften or rejuvenate the recycled binder. This approach is likely subject to evaluation by blending charts. Both approaches are thought to achieve the desired performance grade (PG) of the binder blend based on the assumption that complete blending in fact does occurs between virgin binder, high RAP binder, and RA (if used) during mixing and construction of pavements.

Typical approaches currently used to evaluate changes in binder flow properties due to the addition of recycled binder material to virgin materials is to solvent extract recycled binder material, test rheology (i.e., $G^*/\sin\delta$ and critical temperature) of virgin and extracted binder, then determine rheological properties of both materials after RTFO conditioning. PAV age conditioning of both virgin and recovered material is also required followed by DSR and BBR testing to determine "S" and "m" values for low temperature performance. The critical temperature of recycled-virgin mixtures, in the case of RAP, is then determined as

$$T_{blend} = T_{virgin}(1 - \% RAP) + (\% RAP \times T_{RAP})\tag{1}$$

given

$$T_c(\textbf{high}) = \left(\frac{Log(1) - Log(G^*/\sin\delta @ T_1)}{a = (\Delta Log(G^*/\sin\delta)/\Delta T)}\right) + T_1\tag{2}$$

$$T_c(\textbf{intermediate}) = \left(\frac{Log(5000) - Log(G^*/\sin\delta @ T_1)}{a = (\Delta Log(G^*/\sin\delta)/\Delta T)}\right) + T_1\tag{3}$$

$$T_c(\textbf{S}) = \left(\frac{Log(300) - Log(S_1)}{a = (\Delta Log(G^*/\sin\delta)/\Delta T)}\right) + T_1\tag{4}$$

and

$$T_c(\textbf{m}) = \left(\frac{300 - m_1}{a = (\Delta Log(G^*/\sin\delta)/\Delta T)}\right) + T_1\tag{5}$$

Modelling Neat Binder Composition as it Relates to Rheology

The compositional properties of asphalt, specifically asphaltene content and molecular weight distribution of the maltene and/or oil phase of a binder appear to govern the flow properties of these materials. Hence, asphalt binder flow properties are conveniently described in terms of colloidal suspension theories. Bullard *et al*. [2009] have recently applied differential effective-medium theory (D-EMT) to derive the Pal-Rhodes model of colloidal suspensions. The D-EMT approach considers two conserved forms of the final solution, depending on how the "effective-medium" composite is built up from starting materials. The final conserved solutions to the Pal-Rhodes model are then expressed by [Pauli 2014]

$$\eta_r = \left(1 - K\phi\right)^{-\nu} \tag{6}$$

given

$$\nu = \begin{cases} [\eta] & \phi \le \phi^* \\ [\eta]/K & \phi > \phi^* \end{cases} \tag{7}$$

for some limiting critical volume fraction, ϕ^*.

Regarding asphalt viscosities equations 6 is expressed by

$$\left(\eta/\eta_{nC_7}\right)^{-1/2.5} = 1 - K\chi_{isoC_8} \tag{8}$$

given the following conditions for *K*,

$$K = \begin{cases} 3.3, & \chi \approx< 0.25 \\ <3.3, & \chi \approx> 0.25 \end{cases} \tag{9}$$

which leads to the plot depicted in Figure 1. This figure depicts a plot of $Y \equiv \left(\eta_r \equiv \eta/\eta_{nC_7}\right)^{-1/\nu}$ versus $X \equiv (1 - K\chi_{isoC_8})$, determined for 20 SHRP asphalts where the suspended particle volume fraction ϕ, is approximated by the mass fractions of isooctane insoluble asphaltenes χ_{isoC_8} and heptane soluble maltene viscosities η_{nC_7}. The slope of the line corresponds to a solvation constant, K, determined to be 3.3 for $\eta_r \to 1$ as $\chi_{isoC_8} \to 0$. This correlation is self-consistent suggesting that at $\chi_{isoC_8} = 0, \eta = \eta_0$. Note that $K = 3.3$ limits the maximum asphaltene mass fraction to $\chi_{isoC_8} \le 0.303$, thus the model requires that *K* be an adjustable parameter at higher concentrations.
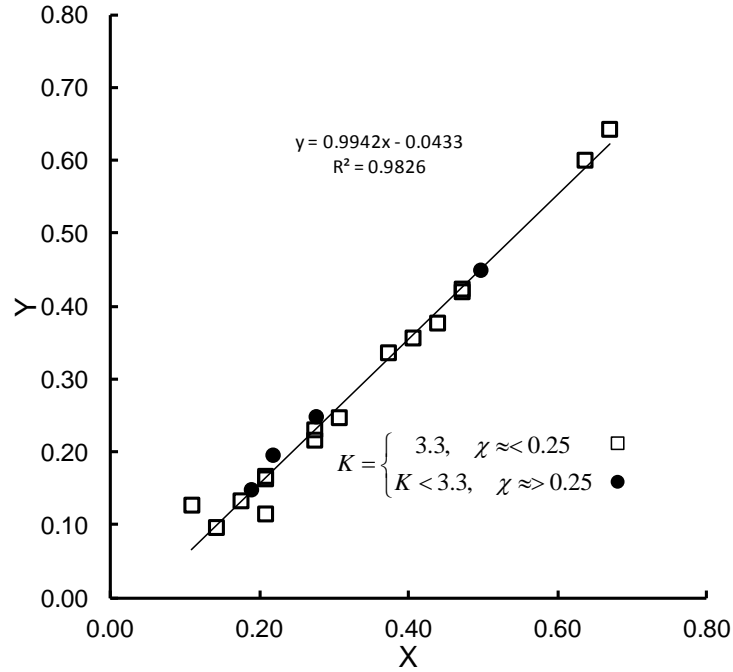
Figure 1. Correlation of relative viscosity function, $Y \equiv \left(\eta / \eta_{nC_7} \right)^{-1/\nu}$ to iso-octane insoluable asphaltene mass fraction, $X \equiv (1 - K\chi_{isoC_8})$, determined for 20 SHRP asphalts.

The concept of asphalt fractions such as asphaltenes and maltenes representing phases in a colloidal suspension may be extended to other types of separation schemes and the material phases generated from them. Bituminous asphalt may for example be separated based on molecular mass or size techniques employing size exclusion chromatography (SEC, also referred to gel-permeation chromatography-GPC) [Branthaver et al. 1993]. The plot in figure 2 shows a direct relationship between the dispersed phase (defined now as high effective molecular weight material) and the elastic nature of the binder defined by the phase angle δ.

The phase angle is derived based on the dynamic viscosity times the frequency of shear $\omega (rad / s)$, which defines the complex modulus $\mathbf{G}^*(\omega)$,

$$\omega \eta^*(\omega) = \mathbf{G}^*(\omega) \tag{10}$$

The complex modulus is a function of the loss (viscous) modulus, $\mathbf{G}''$, and storage (elastic) modulus, $\mathbf{G}'$, such that,

$$\mathbf{G}^*(\omega) = \mathbf{G}'(\omega) + i\mathbf{G}''(\omega) \tag{11}$$

The rheological phase angle is then defined as the inverse tangent of the ratio of the loss (viscous) modulus, $\mathbf{G}''$, to the storage (elastic) modulus, $\mathbf{G}'$,

$$\delta = \tan^{-1}\left(\mathbf{G}''/\mathbf{G}'\right) \tag{12}$$

Variation in the phase angle among asphalts derived from different crude sources is a measure of the elastic-to-viscous character of a viscoelastic medium. In a colloidal suspension this property most likely correlates with properties of the dispersed phase of a suspension. The correlation depicted in figure 2, mathmatically expressed by

$$\frac{\delta}{\left(\delta_0 = 90°\right)} \approx 1 - \chi_{SECI} \tag{13}$$

where $\chi_{SEC-I} \to 0$, as $\delta \to \left(\delta_0 = 90°\right)$, and where $\chi_{SEC-1} \to 1$, as $\delta \to 0$, directly related the dispersed phase of asphalt to the phase angle.
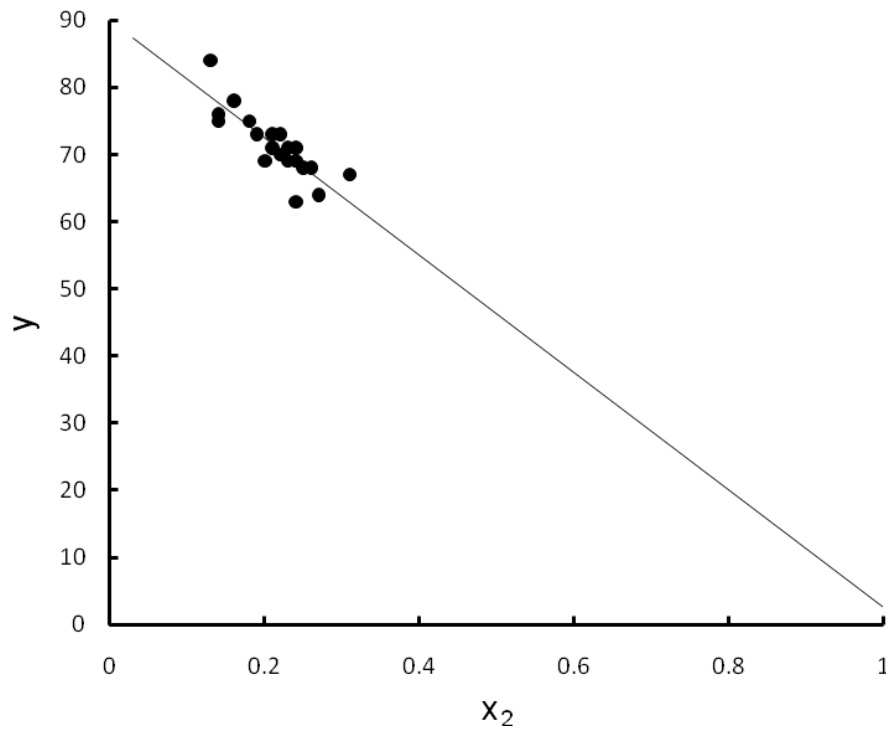

Figure 2. Correlation of phase angle, $y \equiv \delta$ to SEC-I mass fraction, $x_2 \equiv \chi_{SEC-I}$, determined for 20 SHRP asphalts.

EXPERIMENTAL APPROACH

Mix Model of Asphalt Modified with RAP

A simple mixture model of the viscosity of a RAP/asphalt blend may be formulated as

$$\eta_{mix} = x_i \eta_A + (1 - x_i) \eta_R \tag{14}$$

Figure 3 depicts plots of dynamic modulus of virgin asphalt/RAP blends plotted versus mixture dynamic modulus at 15% and 50% by mass RAP content (via equation 14). These figures show a crude source dependence towards the predicted rheological properties.
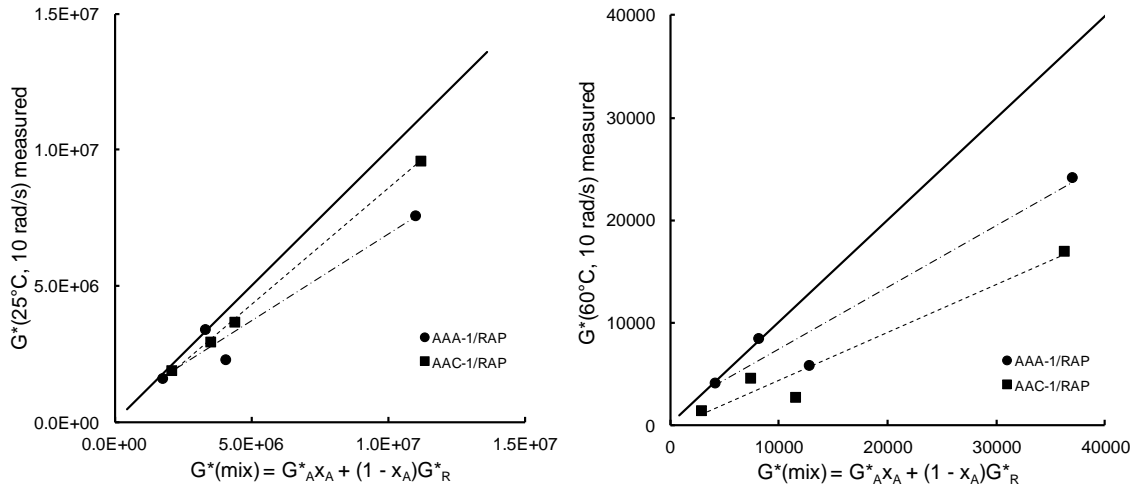

Figure 3. Dynamic modulus of virgin asphalt RAP blends plotted versus mixture dynamic modulus at 15% and 50% by mass RAP content.

If the viscosities of two materials are defined by

$$\eta_A = \eta_{0A}(1 - K\chi_A)^{-2.5} \tag{15}$$

and

$$\eta_R = \eta_{0,R}(1 - K\chi_R)^{-2.5} \tag{16}$$

equation 14 requires a "separation of variables" adjustment (i.e., neat binder asphaltenes mix with RAP asphaltenes and neat binder maltenes mix with RAP maltenes), assuming the validity of the colloidal model presented above. The mix model based on equation 14 is expressed by

$$\eta_{mix} \neq x_i \eta_A + (1 - x_i) \eta_R = x_i \eta_{0A}(1 - K\chi_A)^{-2.5} + (1 - x_i) \eta_{0R}(1 - K\chi_R)^{-2.5} \tag{17}$$

which is not supported by data represented in figure 3. Rather it is observed that the blending rule follows the relationship [Huang and Pauli 2013, Huang et al. 2013],

$$\eta_{mix} = (x_i \eta_{0A} + (1 - x_i) \eta_{0R})(1 - K(x_i \chi_A + (1 - x_i) \chi_R))^{-2.5} \tag{18}$$

Figures 4 depict a plot of maltenes viscosities for two neat binders, their mixture viscosities, blended with two RAP binders at 15% and 50% by mass RAP, plotted versus RAP content. Figure 5 depicts plots of dynamic modulus and phase angle and of two neat asphalts, two RAP binders and their mixtures at at 15% and 50% by mass RAP, plotted versus asphaltene content. These plots support the mixing rule expressed in equation 18.
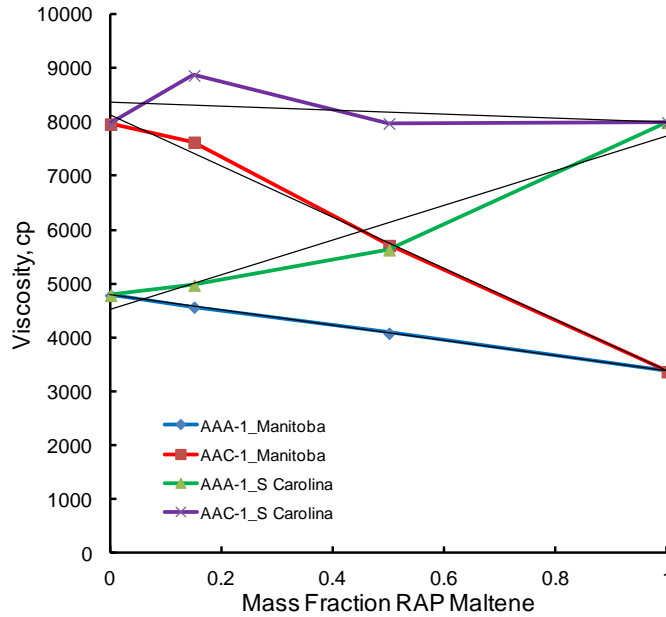

Figure 4. Brookfield viscosities of maltenes of two neat and two RAP binders and of their mixture viscosities at 15% and 50% by Mass RAP plotted versus RAP content.
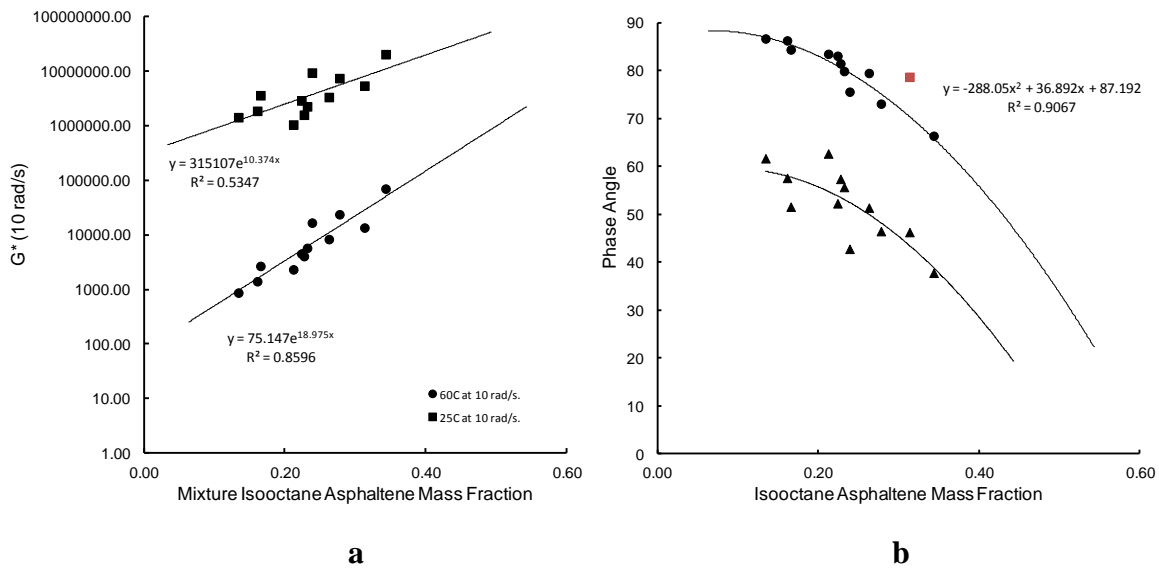

a

b

Figure 5. (a) Dynamic modulus and **(b)** phase angle and of two neat asphalts, to RAP binders and their mixtures at at 15% and 50% by Mass RAP plotted versus asphtene content.

The findings reported here again suggest a "separation of variables" mixing rule where

$$G*_{blend} \propto f(G*_{continuous})g(\chi_{asphaltene})$$ (19)

is required to predict RAP/asphalt binder rheological properties, namely *neat binder asphaltenes mix with RAP asphaltenes and neat binder maltenes mix with RAP maltenes* to more accurately predict the rheological properties of these types of blends.

Automated Flocculation Titrimetry (AFT)

Given that asphalts are viewed by a majority of investigators as colloidal in nature, asphalts derived from different crude sources can be classified as either gel-type (less compatible) or sol-type (more compatible) [Barth 1962; Pfeiffer and Saal 1940]. With "more" compatible asphalts, asphaltenes are usually lower in natural abundance and well dispersed or peptized by the maltene solvent phase. Compatible asphalts also exhibit "more" Newtonian-like flow properties, are more sensitive to temperature change, and generally are more ductile than less compatible asphalts. Conversely, "less" compatible asphalts, relatively speaking, will exhibit more of an elastic property, and hence, are less ductile than compatible asphalts. Based on this description of asphalt compatibility, asphaltene content is one type of measure of compatibility.

Another convenient approach to characterize asphalt compatibility is by defining a state of dispersion of asphaltenes suspended in the maltene phase. Pauli [1996] considered Heithaus compatibility parameters utilizing an automated flocculation titrimetry test. This approach is thought to characterize the suspension-like colloidal stability of asphalt in the bulk phase [Pauli and Branthaver 1998; 1999; Robertson *et al.* 2006; Heithaus 1962]. Heithaus compatibility parameters have long been thought to quantify asphalt "molecular" compatibility, defined as the measure of mutual miscibility among molecular species present in an asphalt system. This is achieved by defining an equilibrium or steady state of a colloidal suspension, also referred to as the state of peptization [Heithaus, 1962].

In the standard Heithaus test individual solutions which vary in concentration containing different masses of asphalt or residuum (W_a) are dissolved in a constant volume of solvent (V_S), usually toluene. These solutions are then titrated with normal alkane solvents, e.g. n-heptane, until flocculation (asphaltene precipitation) is attained. Flocculation onset may be detected by spotting a drop of the solution onto filter paper, resulting in an observable phase separation of precipitated material from material remaining in solution, by use of a microscope, where precipitated material is directly observed, or by automated titrimetric instrumentation. The volume of titrant (V_T) required to initiate flocculation in each solution is used to determine a flocculation ratio (Φ), calculated as $\Phi = V_S/(V_S + V_T)$. Values of flocculation ratio are plotted versus dilution concentration (C), calculated as $C = W_a/(V_S + V_T)$ (Figure 6). A regression line connecting the points is extrapolated to the x and y-axes. The x and y intercepts determined from the extrapolation, referred to as the dilution concentration minimum (C_{min}) and the flocculation ratio maximum (Φ_{max}), respectively, are used to calculate three Heithaus parameters. Heithaus parameters are designated; $p_a = 1 - \Phi_{max}$, which measures the peptizability of the

asphaltene fraction; $p_o = \Phi_{max}(C_{min}^{-1} + 1)$, which measures the solvent power of the maltene fraction, and $P = p_o/(1 - p_a)$, which is a measure of the overall compatibility of the asphalt. Larger values of p_a, p_o, and P generally represent peptizable asphaltenes, maltenes that are a good solvent, and a compatible asphalt overall. Smaller values of p_a, p_o, and P represent the reverse. The p_a and p_o values do not necessarily vary directly with one another among asphalts. An asphalt may be composed of asphaltenes that are not readily peptizable that are dispersed in maltenes that have good solvent characteristics, or the reverse. Table 1 reports "p-values" measured for the eight SHRP asphalt and asphaltene percentages. It is generally noted with the data in this table that n-heptane asphaltene content is linearly correlated with iso-octane asphaltene content, and that asphaltene content is generally inversely proportionally to p_a-values
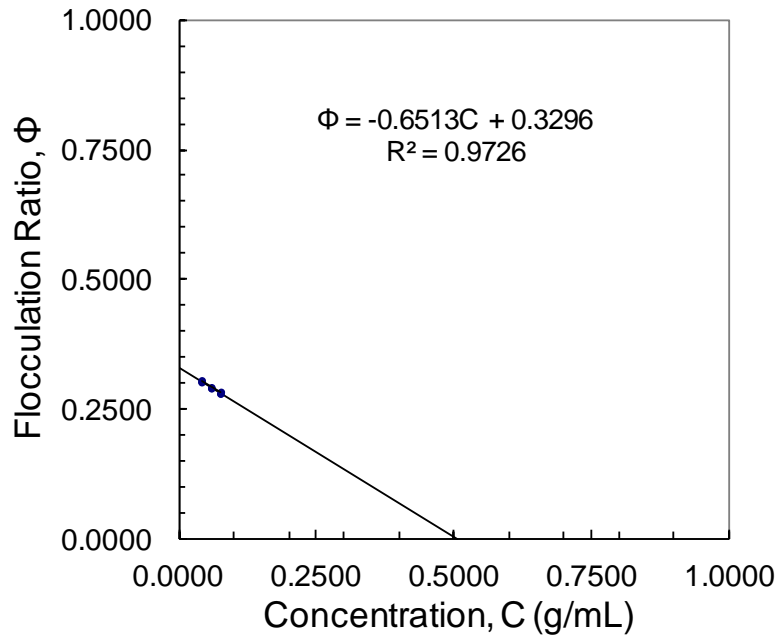

Figure 6. Flocculation ratio versus dilution concentration plot.

Table 1. Heithaus compatibility parameters: asphaltene peptizability (p_a), maltene peptization (p_o), and state of peptization (P) measured by AFT and asphaltene mass fractions based on n-heptane and 2,2,4-trimethylpentane precipitation.

Asphalt	Heithaus asphaltene peptizability parameter, p_a	Heithaus maltene peptization parameter, p_o	Heithaus state of peptization parameter, P	n-Heptane precipitated asphaltene mass fraction	iso-Octane precipitated asphaltene mass fraction
AAA-1	0.701	0.825	2.80	0.158	0.221
AAB-1	0.697	0.872	2.88	0.173	0.224
AAC-1	0.765	0.759	2.23	0.099	0.155
AAD-1	0.660	0.888	2.61	0.202	0.274
AAF-1	0.685	0.732	2.32	0.134	0.187
AAG-1	0.802	0.817	4.12	0.05	0.102
AAK-1	0.692	0.976	3.16	0.201	0.247
AAM-1	0.902	0.759	7.73	0.037	0.112

Flocculation Kinetics Titrimetry (FKT)

Flocculation kinetics titrimetry experiments have been undertaken using automated flocculation titrimetry [Pauli 2004] to measure, among other asphalt compositional properties, asphaltene flocculation rate constants as a function of temperature and concentration and mass percentage of "*flocculation kinetics*" defined asphaltenes.

In FKT testing samples of asphalt are prepared by dissolving specified amounts of asphalt material in toluene, then titrating each solution with iso-octane (2,2,4-trimethyl pentane "isooctane", HPLC Grade). Kinetic experiments are carried out directly after the detection of the flocculation onset (via AFT), at which point in time the addition of titrant is discontinued (i.e., the titrant pump is stopped), but the spectrophotometric monitoring of the test solution is allowed to continue. This approach allows for the measurement in the change in absorption of UV-Visible light, monitored at a frequency of 740 nm, over time. Plots of the change in absorption of UV-Visible light at 740 nm versus time are then used to characterize the kinetic process of asphaltenes precipitating from solution, constituting a measure of the rate of flocculation.

A second-order rate equation

$$\frac{dc_A}{dt} \approx -k_1 c_A{}^2 . \tag{20}$$

models the forward process of the reaction mechanism

$$A_j + A_i \xrightarrow{\ k_{ij}\ } A_{j+i} , \tag{21}$$

assuming that the flocculation process involves both conduction and diffusion of A_i-monomer asphaltene molecules attaching to A_j-mer clusters already present in a colloidal solution.

Limits of integration are imposed on equation 20 when taking into account the material balance of "*what species have and have not flocculated*", resulting in initial and final solution concentrations of $c_{\infty,s\ln} = (1/V)(n_{max} - n_{\infty,agg})$, and $c_{0,s\ln} = (1/V)(n_{max} - (n_{0,agg} = 0))$, respectively. These two material balance limits are defined by V, the total volume of solution and $n_{0,agg}$, n_{max}, and $n_{\infty,agg}$, which define the number of moles of solute particles, initially in solution, the maximum number of moles which may potentially flocculate, and the number of moles which actually are observed to flocculate. The integral,

$$\int_{c_{0,s\ln}}^{c_{\infty,s\ln}} \frac{dc_A}{c_A^{\,2}} = -\int_{t_0=0}^{t_\infty} kdt \tag{22}$$

once evaluated, defines the time-dependent concentration of flocculated asphaltenes $c_A(t)$, in terms of the rate constant k, time t, and a steady-state concentration $c_{A\max}$, expressed as

$$c_A(t) = c_{A\max} - \frac{c_{A\max}}{1 + c_{A\max}kt} \tag{23}$$

where

$$(Abs_{adj})_{max} = \delta l c_{A\max} \tag{24}$$

given the path length of the flow cell l, and the molar extinction coefficient δ. A flocculation-rate curve (depicted in figure 7) is derived from flocculation kinetics plots by truncating both absorption and time data to a literal "0" value (i.e., at the flocculation onset, effectively initiating the flocculation reaction).
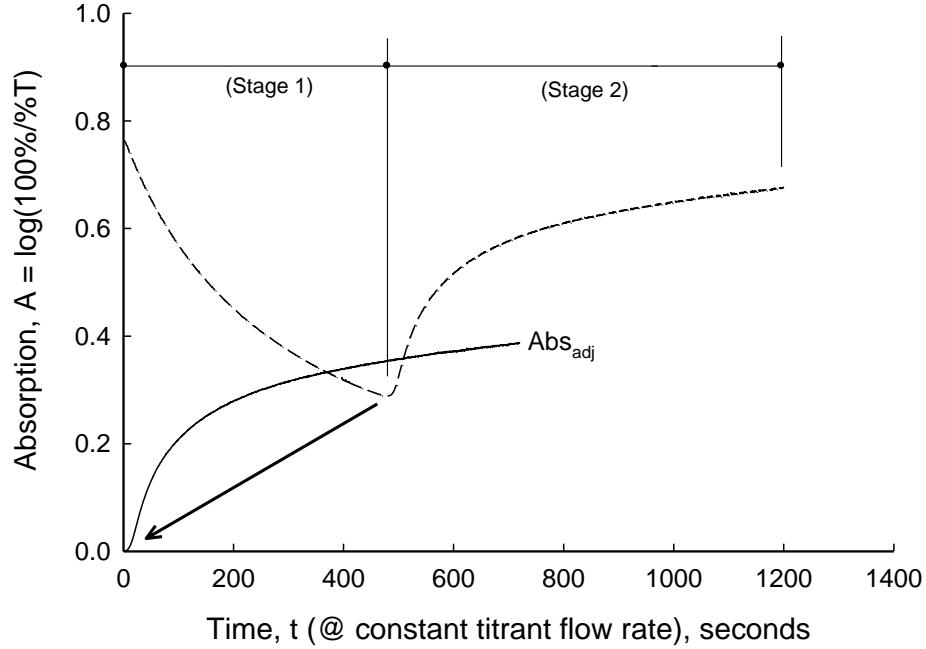
Figure 7. Absorption versus time (seconds) plot for SHRP asphalt AAA-1. Dash–curve: flocculation onset curve (Stage 1) plus rate curve (Stage 2) measured at initial concentration; c_0 = 0.250 g/mL, T = 25°C. Solid-curve: truncated rate curve.

An initial adjusted absorption, $(Abs_{adj})_{initial}$, and an initial adjusted time, $(t_{adj})_{initial}$, are calculated by subtracting the absorption and time values at the flocculation onset from all preceding absorption and time data points. This step effectively translated the flocculation-rate curve to $(Abs_{adj})_{initial} = 0$ and $(t_{adj})_{initial} = 0$ prior to fitting of the data to the following equation

$$Abs(t_{adj}) = (Abs_{adj})_{max} - \frac{(Abs_{adj})_{max}}{1 + (Abs_{adj})_{max} k t_{adj}}$$

(25)

where $(Abs_{adj}) \propto c_A$, and $(Abs_{adj})_{max} \propto c_{A\,max}$.

Flocculation kinetics plots are generated based on a calculated flocculation rate constant k, derived in terms of the effective amount of blocked light $(Abs_{adj})_{max}$, measured at 740 nm through a small path length flow cell, which may be correlated with the amount of normal heptane asphaltene mass fractions $\chi_{n\text{-}heptane}$, determined by a solvent de-asphaltene separation method [Branthaver et al. 1991].

Figure 8 depicts a plot of $(Abs_{adj})_{max}$ versus $\chi_{n\text{-}heptane}$ data at two concentration levels, each fitted to a correlation function of the form

$$\left[(Abs_{adj})_{max}(c_0) \right]_{T,P} = \beta_0 + \beta_1 \chi_{n-heptane} + \beta_2 \chi_{n-heptane}^2$$
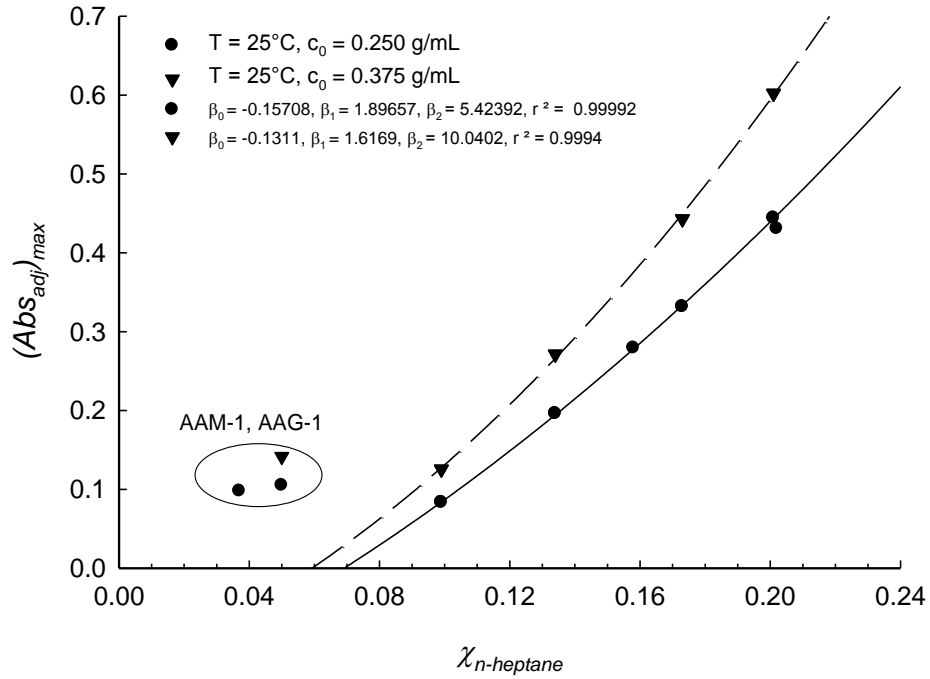
(26)

Figure 8. Maximum absorption of flocculated material plotted as a function of the n-heptane insoluble asphaltene mass fraction, determined for 0.250 g/mL and 0.375 g/mL solutions of asphalt prepared in toluene and titrated with iso-octane at 25°C.

From a phenomenological point-of-view the principle reaction [Benson 1960; Atkins 1994; Levine 1988; Steinfeld et al. 1999]

$$A_j + A_i \xrightarrow{\ k_{ij}\ } A_{j+i}, \tag{27}$$

assumes a process involving both conduction and diffusion of A_i-monomer asphaltene molecules attaching to A_j-mer clusters already present in a colloidal solution, forming A_{j+i} flocculated particle clusters. The particle flux, $J_i = -D_i\left(dc_i/dR\right)$, is then defined as the concentration c_i, of A_i-monomer molecules migrating through a hypothetical spherical surface element $4\pi R_{ji}^{\ 2}$, such that the rate of exchange in the number of moles of A_i-monomer molecules per unit time dn_i/dt, is expressed by

$$\frac{dn_i}{dt} = 4\pi R_{ji}^{\ 2} D_{ij} \frac{dc_i}{dR_{ji}} \tag{28}$$

Here $R_{ji} = r_j + r_i$ defines the intra-molecular distance between A_j-mer clusters and A_i-monomer molecules, respectively, once in contact, and the term $(D_{ji} \equiv D_i + D_j)$ represents the effective diffusion coefficient for "reactants" A_i and A_j. Integration of equation 28

$$\int_{c_{i,R=r_i+r_B}}^{c_{i,R=\infty}} dc_B = \frac{dn_i}{dt} \frac{1}{4\pi(D_i + D_j)} \int_{R_{ji}=r_j+r_i}^{\infty} \frac{dR}{R^2} \tag{29}$$

between the limits; "*of when all available clusters and molecules are in contac*t" ($R_{ji} = r_j + r_i$,), and "*when they are in solution (at infinite separation at R = ∞)*", results in the difference in concentration for time-initial and time-final expressed by

$$c_{i,R\to\infty} - c_{i,R_{ji}} = \frac{dn_i}{dt} \frac{1}{4\pi D_{ji} R_{ji}}, \tag{30}$$

Imposing the following steady-state conditions in terms of the number of *j*-mer particles, N_j. [Levine 1988], namely

$$\frac{dn_i}{dt} = \frac{kc_j c_i V}{N_j} = \frac{kc_j c_i V}{N_A n_j} = \frac{kc_j c_i}{N_A c_j} = \frac{kc_i}{N_A} \tag{31}$$

the rate per unit molecular volume, $\bar{v}$, describing this "bimolecular" reaction is shown to be related to the forward rate constant *k*, and the concentrations of suspended clusters and molecules as

$$\frac{N_j dn_i}{V dt} \equiv \bar{v} = kc_j c_i, \tag{32}$$

Substitution of equation 32 into 31, then into equation 30, with some rearrangement gives

$$c_{i,R} = c_i \left(1 - \frac{k}{4\pi N_A D_{ji} R_{ji}} \right) = \left(1 - \frac{k}{k_{diff}} \right) \tag{33}$$

Thus, an expression defining the diffusion-limited rate constant is defined by

$$4\pi N_A D_{ji} R_{ji} = k_{diff} \tag{34}$$

where N_A is Avogadro's number.

If the Stokes-Einstein [Levine 1988] equation, defining the diffusion coefficient,

$$D_{si}^{\infty} = \frac{k_B T}{6\pi\eta_s r_j} \tag{35}$$

is the substituted into 34, given k_B Boltzmann's constant, and η_s the solvent viscosity, and given the approximation that ($1/2R_{ji} = r_j = r_i$,) [Atkins 1994], and the substitution of $N_A k_b = R$, where R is the ideal gas constant, an expression relating the solution viscosity to the diffusion-limited rate constant k_{diff}, may be expressed by

$$k_{diff} = 4\pi N_A R_{ji} \left(\frac{k_B T}{3\pi\eta_s R_{ji}} + \frac{k_B T}{3\pi\eta_s R_{ji}} \right) = \frac{8RT}{3\eta_s} \tag{36}$$

Equation 36 defines an ideal diffusion-controlled process relationship (i.e., $8RT/3\eta_s = k_{diff}$) relating the viscosity of the solvent phase of a colloidal suspension to the rate constant of diffusing particles in the suspension. Figures 9 and 10 depict the relationship between the asphaltene flocculation rate constant and the maltene viscosity for several experimental data sets derived from testing the 8 SHRP core asphalts.
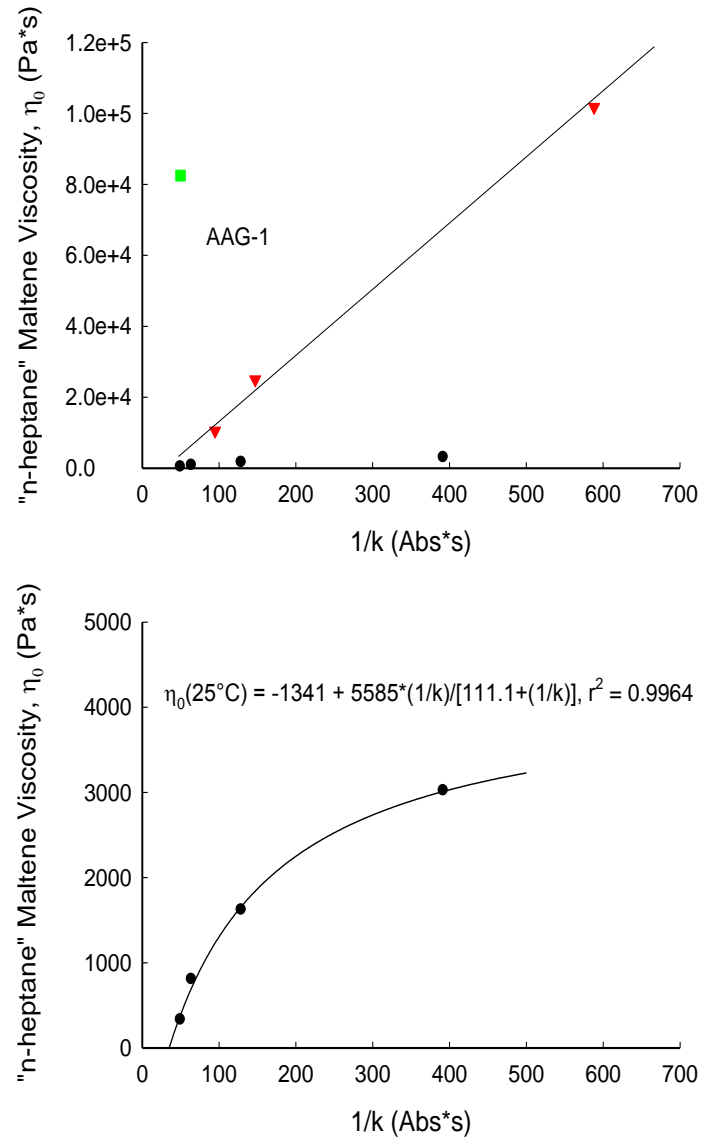
Figure 9. n-Heptane soluble maltene fraction viscosities (Pa*s @ 25°C) plotted versus the inverse of the rate constant of flocculation, measured at 25°C. Top plot depicts eight SHRP asphalts with correlation line drawn through "higher viscosity maltenes" asphalts, and bottom plot depicts four of the eight SHRP asphalts with correlation line drawn through "low viscosity maltenes" asphalts.
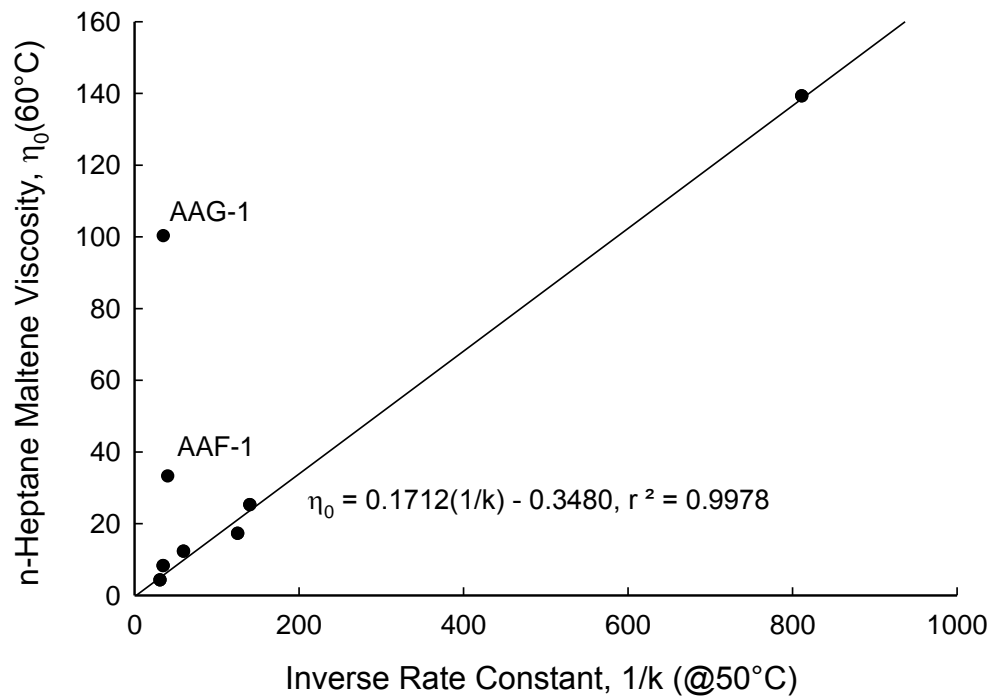
Figure 10. "n-Heptane-Soluble Maltenes Fraction" viscosities (Pa*s @ 60°C) plotted versus the inverse of the flocculation rate constant measured at 50°C.

RESULTS AND DISCUSSION

Asphalt samples were prepared as 0.600 g and 0.800 g per 3.0 mL toluene solutions. Sample solutions, after sitting for 24-h, were titrated with 2,2,4-trimethylpentane (iso-octane) at a rate of 0.300 mL/min and at a temperature of 35°C. At the detection of the flocculation onset (figure 11) 30-seconds of additional titrant was added to the solution, then the titrant was discontinued. The flocculation of asphaltenes was then monitored for 10-minutes.
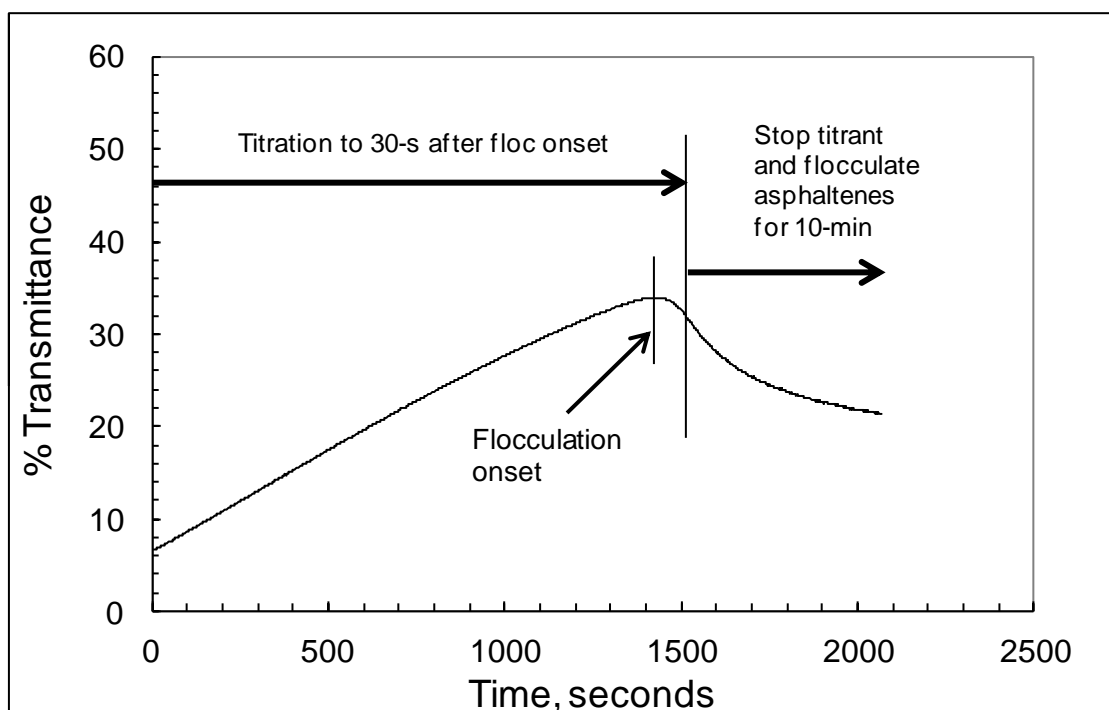
Figure 11. Percent transmittance versus titrant delivery time AFT flocculation plot.

Compatibility parameters and flocculation kinetics parameters were determined for each set of 0.600 g and 0.800 g asphalt per 3.0 mL toluene data (figures 12 and 13).

Directly after completion of a titration/flocculation test, the test solution was removed from the AFT instrument and diluted with an additional 20-mL of iso-octane. Sample vials were capped and stored away to be filtered at a later time.

AFT solutions were filtered with tared 10-micron filter paper through a Buchner funnel. Filter paper with filter cake asphaltenes were dried in a 75°C oven for a 1-hr prior to determining the final weight of asphaltenes recovered.

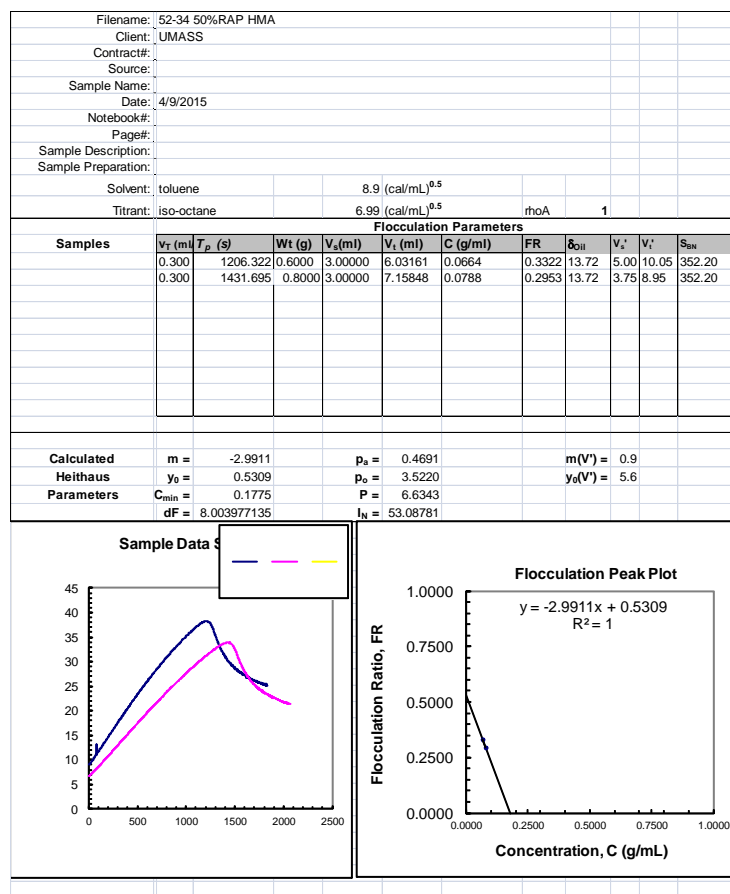|											
Filename:	52-34 50%RAP HMA										
Client:	UMASS										
Contract#:											
Source:											
Sample Name:											
Date:	4/9/2015										
Notebook#:											
Page#:											
Sample Description:											
Sample Preparation:											
Solvent:	toluene			8.9	$(cal/mL)^{0.5}$						
Titrant:	iso-octane			6.99	$(cal/mL)^{0.5}$		rhoA	1			

Flocculation Parameters

Samples	v_T (ml)	T_p (s)	Wt (g)	V_s(ml)	V_t (ml)	C (g/ml)	FR	δ_{Oil}	V_s'	V_t'	S_{BN}
	0.300	1206.322	0.6000	3.00000	6.03161	0.0664	0.3322	13.72	5.00	10.05	352.20
	0.300	1431.695	0.8000	3.00000	7.15848	0.0788	0.2953	13.72	3.75	8.95	352.20

Calculated	m =	-2.9911		p_a =	0.4691		m(V') =	0.9
Heithaus	y_0 =	0.5309		p_o =	3.5220		y_0(V') =	5.6
Parameters	C_{min} =	0.1775		P =	6.6343			
	dF =	8.003977135		I_N =	53.08781			

Sample Data S[...]

Flocculation Peak Plot

y = -2.9911x + 0.5309
R² = 1

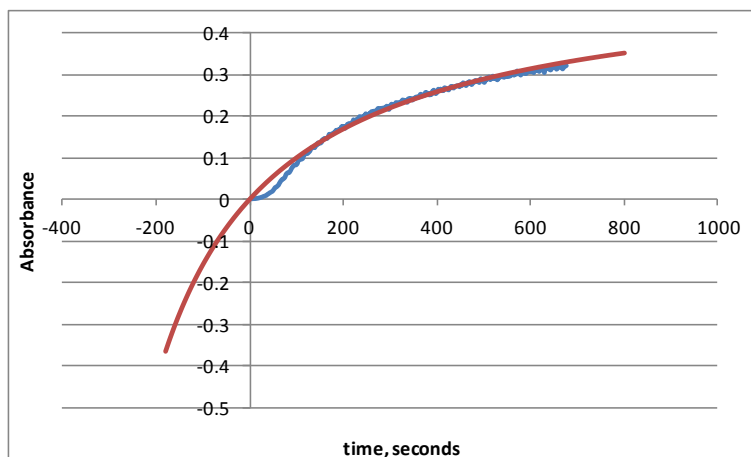**Figure 12.** AFT Heithaus [Heithaus 1962] compatibility worksheet.

Figure 13. FKT asphaltene flocculation rate plot fit to the expression

$$Abs(t_{adj}) = (Abs_{adj})_{\max} - \left[(Abs_{adj})_{\max} \Big/ \left(1 + (Abs_{adj})_{\max} k t_{adj}\right) \right].$$

Table 2 reports AFT and FKT parameters determined for 10 UMASS binder samples. Plots depicted in Figure 14 show a correlation plot relating the maximum absorbance, derived based on equation 25, to asphaltene mass percentage determined gravimetrically. Linearity between $(Abs_{adj})_{max}$ and $100 \cdot \chi_{asphaltenes}$ is observed within the concentration range of 15% to 24% asphaltenes. The flocculation test is based on detection of blocked light in a concentrated solution, thus, the cell path length and differences in light absorption characteristic of the sample likely bias the test resulting in the limited concentration range of correlation.

Table 2. AFT and FKT parameters determined for 10 UMASS binder samples.

Sample	p_a	p_o	P	Abs (0.8-g)	k(0.8-g)	% asphaltene
64-28 Control	0.35	4.98	7.72	0.521	4.39E-03	4.8
64-28 15%RAP HMA	0.46	3.26	6.02	0.519	4.71E-03	16.9
64-28 25%RAP HMA	0.62	1.28	3.34	0.548	4.06E-03	24.2
64-28 35%RAP HMA	0.57	1.84	4.27	0.615	4.55E-03	24.5
64-28 50%RAP HMA	0.58	1.89	4.50	0.549	3.45E-03	24.0
RAP Stockpile Material	0.62	1.55	4.07	0.527	3.17E-03	20.0
64-28 50%RAP WMA	0.70	0.15	0.50	0.561	3.11E-03	20.6
64-28 35%RAP WMA	0.62	1.11	2.95	0.503	4.43E-03	17.8
52-34 50%RAP HMA	0.47	3.52	6.63	0.452	2.99E-03	20.1
52-34 35%RAP HMA	-1.16	28.23	13.08	0.496	2.11E-03	23.4

A predicted asphaltene concentration may be calculated for mixtures of two binders (neat binder blended with a RAP binder for example) in the absence of oxidation of the material blend during mixing, utilizing the following equation

$$\chi_{mix} = \left(x_i \chi_A + \left(1 - x_i\right) \chi_R \right) \tag{37}$$

Table 3 reports predicted asphaltene concentration based on the asphaltene contents of the original materials (i.e., control and RAP stockpile material) and the percentage of RAP. Figure 15 depicts a plot relating gravimetric asphaltenes and predicted blend asphaltenes to RAP percentage in a mix. Assuming that HMA materials undergo more extensive oxidation during the mixing process compared to WMA material, both these materials are observed to have substantially higher asphaltene contents (presumed to be due to mix plant condition oxidation) compared to predicted values.

Table 3. Predicted asphaltene content based on mix model (Eq 37).

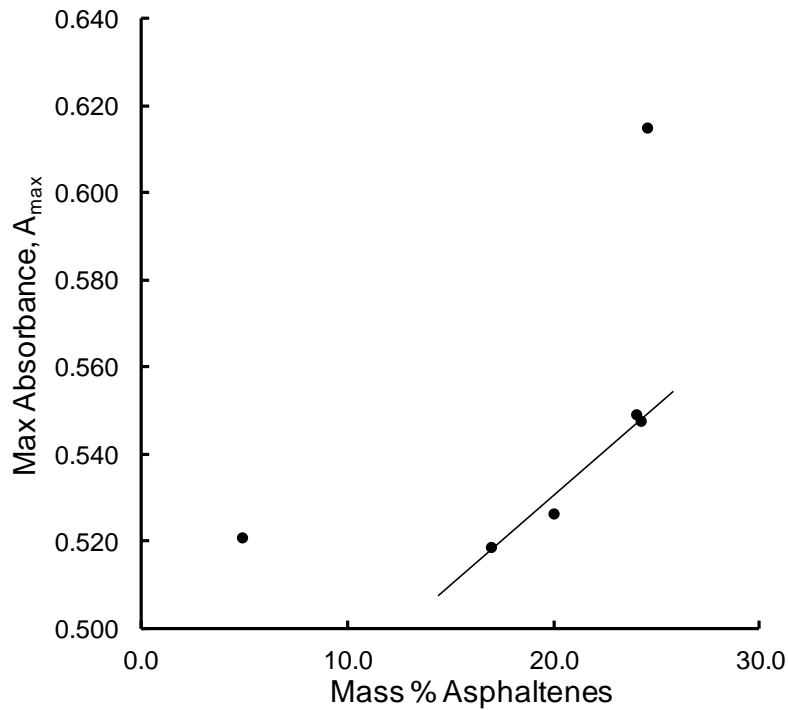| Sample	%RAP	% Asphaltene 0.8g	Mix Asphaltenes
64-28 Control	<u>**0**</u>	<u>**4.8**</u>	4.8
64-28 15%RAP HMA	<u>**15**</u>	16.9	7.1
64-28 25%RAP HMA	<u>**25**</u>	24.2	8.6
64-28 35%RAP HMA	<u>**35**</u>	24.5	10.1
64-28 50%RAP HMA	<u>**50**</u>	24.0	12.4
RAP Stockpile Material	<u>**100**</u>	<u>**20.0**</u>	20.0

Figure 14. Correlation plots relating maximum absorbance to asphaltene mass percentage determined gravimetrically.
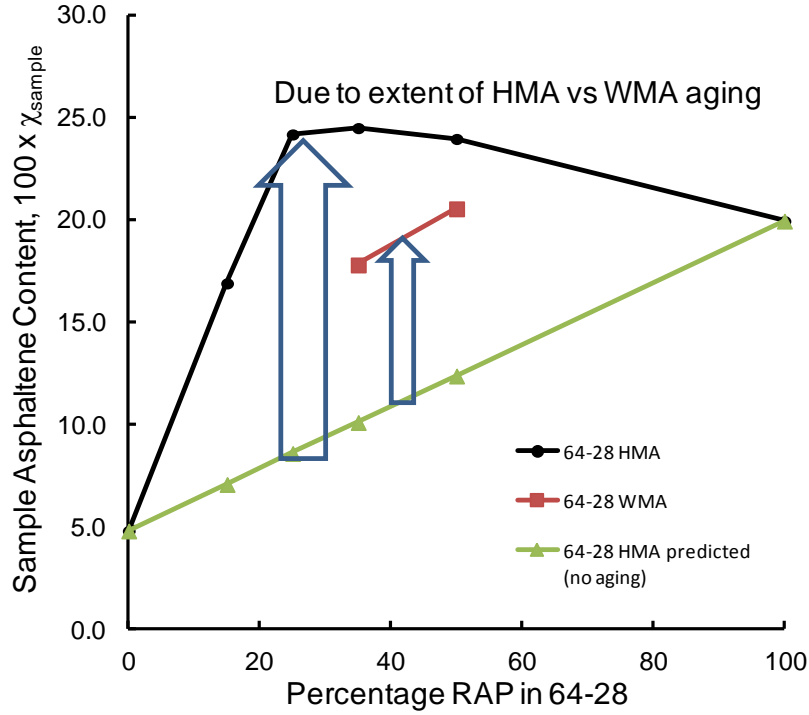
Figure 15. Plots relating gravimetric asphaltenes to RAP percentage in a mix.

Utilizing FKT data it is possible to predict maltene viscosities: Furthermore, if both maltene viscosities and asphaltene content of a blend are known it is possible to predict the binder viscosities. The following line of reasoning is employed:

Given the flocculation rate constants k, and assuming identical size particle formation and interaction during the flocculation testing, (i.e., $\xi = \text{constant} = 1$), flocculating solution viscosities are calculated as

$$\eta_s(k) = \xi \frac{1}{k} \tag{38}$$

The flocculation solution is then related to the viscosities of the solution component viscosities as

$$\eta_s(k) = \phi_{titrant}\eta_{titrant} + \phi_{solvent}\eta_{solvent} + \phi_{maltene}\eta_{maltene} \tag{39}$$

Next, the maltene volume fraction is approximated by $\phi_{maltene} \approx (1 - \chi_{asphaltene})$ given the asphaltene mass fraction $\chi_{asphaltene} = 0.01(Mass\ \%\ asphaltenes)$ and ignoring differences in density among samples, such that the viscosity of the maltene fraction of a tested binder is calculated as

$$\eta_{maltene} = \frac{1}{\phi_{maltene}}\left(\eta_s(k) - \left(\phi_{titrant}\eta_{titrant} + \phi_{solvent}\eta_{solvent}\right)\right) \tag{40}$$

where

$$\phi_i = \frac{V_i}{V_i + V_j + V_k} \tag{41}$$

It is further assumed that the viscosity of the test solvents (titrant + solvent) in the solution is much less than the maltene viscosity,

$$\eta_{maltene} > \eta_s(k) \, \square \, \left(\phi_{titrant}\eta_{titrant} + \phi_{solvent}\eta_{solvent}\right) \tag{42}$$

thus

$$\eta_{maltene} \approx \frac{\eta_s(k)}{\phi_{maltene}} \tag{43}$$

Finally, the viscosity of the binder, based on the Pal-Rhodes equation is calculated as

$$\eta_{blend} = \eta_{maltene}(1 - 3.3\chi_{asphaltene})^{-2.5} \tag{44}$$

Table 4 reports AFT and FKT parameters used to calculate predicted maltene viscosities and predicted binder viscosities for 64-28 HMA blends, the control and the RAP material. Maltene viscosities based on a mixing rule

$$\left(\eta_{malt}\right)_{mix} = \left(x_i\eta_{0A} + (1-x_i)\eta_{0R}\right) \tag{45}$$

were also compared with maltene viscosities determined based on flocculation rates. Figure 16, which depicts a plot of maltene viscosities based on the mix rule (Eq 45) compared with maltene viscosities based on flocculation rate constants (Eq 43) show these values to reasonably line up in one:to:one correspondence, unlike predicted and measured asphaltenes.

A notable peculiarity may be pointed for measured p-values for the 64-28 Control as compared to typical p-values of SHRP when data in tables 1 and 2 are compared. It has been generally noted that p_a values decrease and p_o values increase with increasing oxidation of a binder. It has also been observed in other types of heavy residuum that high p_o values (>1.5) are indicative of high concentration of polar aromatics, and sometimes non-organic particulate matter. Based on the resulted reported in table 2 for the 64-28 Control sample, material blends with RAP after mix plant conditions appear to result in excessive oxidation, and hence, excessive asphaltene

production. As a result of this, predicted viscosities of the blends may be observed to be much higher than predicted based on a simple mixture formulation, as depicted in Figure 17.

Table 4. AFT and FKT parameters determined for 10 UMASS binder samples.

Sample	$V_{solvent}\ (mL)$	$V_{titrant}\ (mL)$	$\phi_{solvent}$	$\phi_{solvent}$	$\phi_{titrant}$	$\eta_{maltene}$
64-28 Control	3	7.02	0.278	0.651	0.071	**<u>3225</u>**
64-28 15%RAP HMA	3	6.54	0.294	0.641	0.065	3263
64-28 25%RAP HMA	3	6.69	0.291	0.650	0.059	4184
64-28 35%RAP HMA	3	6.57	0.295	0.646	0.059	3698
64-28 50%RAP HMA	3	6.97	0.284	0.659	0.058	5035
RAP Stockpile Material	3	7.34	0.273	0.669	0.058	**<u>5416</u>**

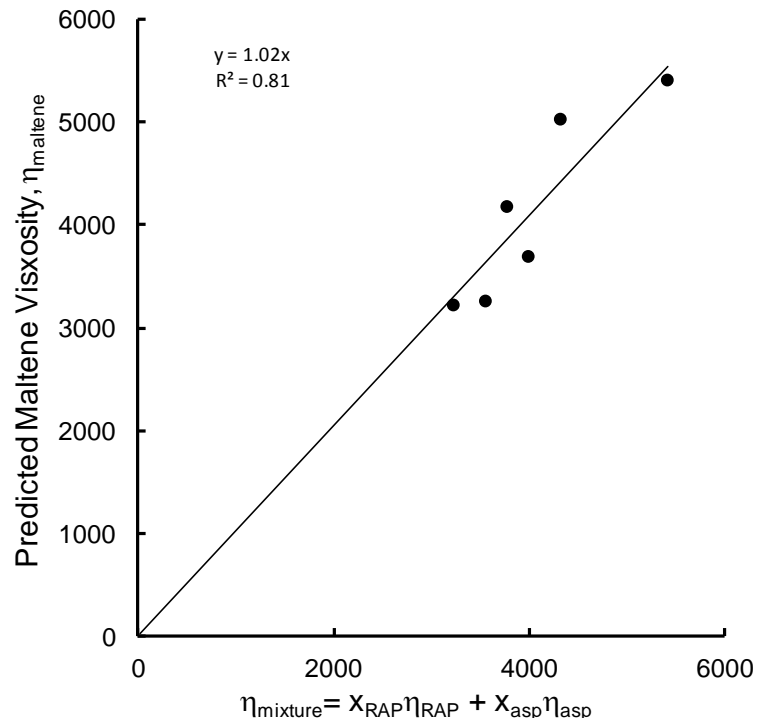| Sample	$1/k = \eta(k)$	$\left(\eta_{malt}\right)_{mix}$	$\eta = \eta_m(1-3.3\chi_{mix})^{-2.5}$	$\eta = \eta_m(1-3.3\chi_a)^{-2.5}$
64-28 Control	228	3225	4975	4975
64-28 15%RAP HMA	213	**<u>3553</u>**	6922	27364
64-28 25%RAP HMA	246	**<u>3773</u>**	8697	205558
64-28 35%RAP HMA	220	**<u>3992</u>**	11024	247661
64-28 50%RAP HMA	290	**<u>4320</u>**	16075	215515
RAP Stockpile Material	316	5416	79376	79376

Figure 16. Maltene viscosities based on a mix rule compared with Maltene viscosities based on flocculation rate constants.

Table 1. Heithaus compatibility parameters: asphaltene peptizability (p_a), maltene peptization (p_o), and state of peptization (P) measured by AFT and asphaltene mass fractions based on n-heptane and 2,2,4-trimethylpentane precipitation.

Asphalt	Heithaus asphaltene peptizability parameter, p_a	Heithaus maltene peptization parameter, p_o	Heithaus state of peptization parameter, P	n-Heptane precipitated asphaltene mass fraction	iso-Octane precipitated asphaltene mass fraction
AAA-1	0.701	0.825	2.80	0.158	0.221
AAB-1	0.697	0.872	2.88	0.173	0.224
AAC-1	0.765	0.759	2.23	0.099	0.155
AAD-1	0.660	0.888	2.61	0.202	0.274
AAF-1	0.685	0.732	2.32	0.134	0.187
AAG-1	0.802	0.817	4.12	0.05	0.102
AAK-1	0.692	0.976	3.16	0.201	0.247
AAM-1	0.902	0.759	7.73	0.037	0.112

Table 2. AFT and FKT parameters determined for 10 UMASS binder samples.

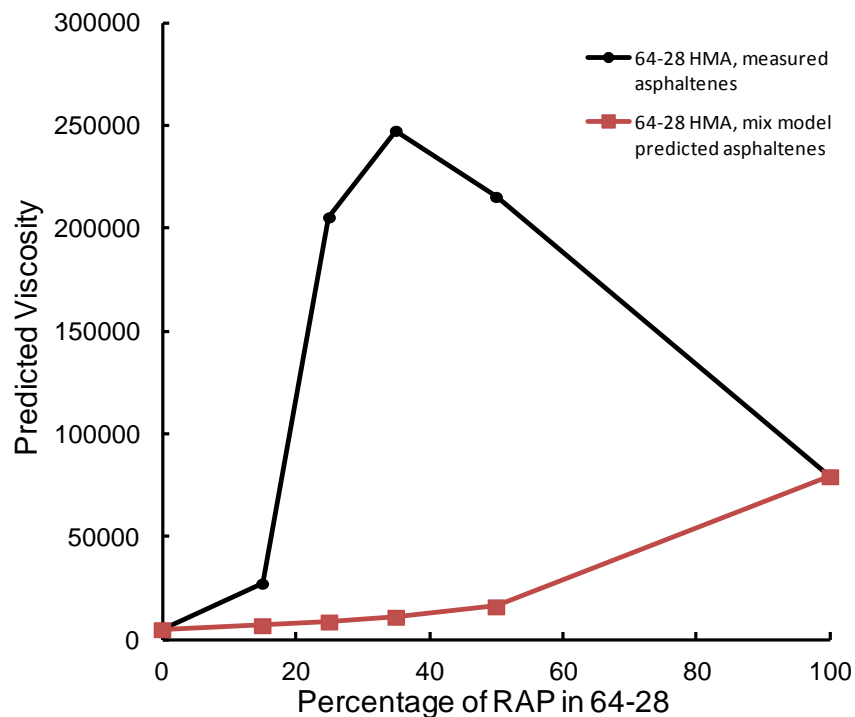| Sample	p_a	p_o	P	Abs (0.8-g)	k(0.8-g)	% asphaltene
64-28 Control	0.35	4.98	7.72	0.521	4.39E-03	4.8
64-28 15%RAP HMA	0.46	3.26	6.02	0.519	4.71E-03	16.9
64-28 25%RAP HMA	0.62	1.28	3.34	0.548	4.06E-03	24.2
64-28 35%RAP HMA	0.57	1.84	4.27	0.615	4.55E-03	24.5
64-28 50%RAP HMA	0.58	1.89	4.50	0.549	3.45E-03	24.0
RAP Stockpile Material	0.62	1.55	4.07	0.527	3.17E-03	20.0
64-28 50%RAP WMA	0.70	0.15	0.50	0.561	3.11E-03	20.6
64-28 35%RAP WMA	0.62	1.11	2.95	0.503	4.43E-03	17.8
52-34 50%RAP HMA	0.47	3.52	6.63	0.452	2.99E-03	20.1
52-34 35%RAP HMA	-1.16	28.23	13.08	0.496	2.11E-03	23.4

Figure 17. Predicted binder viscosities based on mix model calculations.

CONCLUSIONS AND RECOMMENDATIONS

Evaluation of the compatibility parameters measured specifically for the 64-28 data sets suggests that the RAP Stockpile Material is characterized by typical p-values for a mildly aged binder material, but the 64-28 Control material (Base binder) is measured to have atypical p-values, specifically, the low p_a value is more often characteristic of high asphaltene content, but in the present case asphaltene content is low, and high p_o values are indicative of high concentrations of polar aromatic materials, and or a more complex chemical make (polymer or other type of modification) than is typical for a straight run binder. It was further noted that the increase in asphaltene content for RAP blends was related to simulated mix plant conditioning, thus it was observed that 64-28 WMA materials at the same RAP content showed less asphaltene content than 64-28 HMA materials. It is speculated based on the results presented that this particular blend of 64-28 Control material with RAP is highly susceptible to mix plant condition oxidation. Blending theories of residua also suggest that blending of materials with vastly different compatibility characteristics may lead to very incompatible resultant blends.

Additional testing may involve IR-spectrometric investigation to evaluation the extent of oxidation and to better characterize the starting and blended materials. Chromatographic separation (SARA, GPC, IEC) and material fraction physicochemical characterization (IR) of the 64-28 Control material may also provide additional information regarding this material's

peculiar compatibility characteristics. Atomic force microscopic (AFM) studies may also provide further information regarding wax content, polymer modification, and presence of recycled motor oil bottoms.

References

ASTM D6703-07, 2010, Standard Method for Automated Heithaus Titrimetry. Annual Book of ASTM Standards, Road and Paving Materials; Vehicle-Pavement Systems, Section 4, vol. 04.03. ASTM International, West Conshohocken, PA.

Atkins, P.W., 1994, Physical Chemistry Fifth Edition. Oxford University Press, Oxford ENGLAND.

Barth, E. J., 1962, Asphalt Science and Technology, Gordon and Breach Science Publishers, New York.

Benson, S. W., 1960, The Foundations of Chemical Kinetics, McGraw-Hill, Inc., New York.

Branthaver, J. F., J. C. Petersen, R. E. Robertson, J. J. Duvall, S. S. Kim, P. M. Harnsberger, T. Mill, E. K. Ensley, F. A. Barbour, and J. F. Schabron, 1993, SHRP-A-368, Binder Characterization and Evaluation, Volume 2: Chemistry. Strategic Highway Research Program, National Research Council, Washington, DC.

Branthaver, J. F., J. C. Petersen, J. J. Duvall, and P. M. Harnsberger, 1991, Compatibilities of Strategic Highway Research Program Asphalts. Transportation Research Record 1323, 22-31.

Bullard, J. W., A. T. Pauli, E. J. Garboczi and N. S. Martys, 2009, A Comparison of Viscosity-Concentration Relationships for Emulsions. J. Colloid Interface Sci., 330 (1), 186-193.

Heithaus, J. J., 1962, Measurement and Significance of Asphaltene Peptization. Journal of the Institute of Petroleum, 48, 45-53.

Huang, Shin-Che and A.T. Pauli, Physicochemical Characteristics of RAP Blend Binders, Submitted to the 12th ISAP Conference on Asphalt Pavements, Raleigh, North Carolina, August, 2013.

Huang, Shin-Che, T. Pauli, W. Grimes, and F. Turner, "Aging Characteristics of RAP Binder Blends-What Types of RAP Binders are Suitable for Multiple Recycling?" accepted for presentation and publication at the Journal of Association of Asphalt Paving Technologist for consideration for publication and presentation, August, 2013.

Levine, I. N., 1988, Physical Chemistry, 3rd Ed., McGraw-Hill, Inc, New York.

McDaniel, R., H. Soleymani, M. Anderson, P. Turner, and R. Peterson, 2000. Recommended Use of Reclaimed Asphalt Pavement in the SuperPave Mixture Design Method. NCHRP Report 452, TRB, Washington, DC,

Pauli, Adam T., 1996, Asphalt compatibility testing using the automated Heithaus titration test. Preprints of Papers - American Chemical Society, Division of Fuel Chemistry, 41(4), 1276-1281.

Pauli, Adam T., 2004, A study of the rates of flocculation of asphaltenes in asphalt-solvent solutions measured by automated flocculation titrimetry. Preprints - American Chemical Society, Division of Petroleum Chemistry, 49(2), 135-137.

Pauli, A. T., 2014, Chemomechanics of Damage Accumulation and Damage Recovery Self-Healing in Bituminous Asphalt Binders. Dissertation, Printed by Sieca Repro, Delft, The Netherlands. ISBN 978-94-6186-269-3.

Pauli, A. T., and J. F. Branthaver, 1998, Relationship Between Asphaltenes, Heithaus Compatibility Parameters and Asphalt Viscosity. Petroleum Science and Technology, 16(9&10): 1125-1147.

Pauli, A. T., and J. F. Branthaver, 1999, Rheological and Compositional Definitions of Compatibility as They Relate to the Colloidal Model of Asphalt and Residua. American Chemical Society Division of Petroleum Chemistry Preprints, 44, 190-193.

Pfeiffer, J. P., and R. N. J., Saal, 1940, Asphalt Bitumen as Colloidal System. Phys. Chem., 44, 139-149.

Robertson, R. E., K. P. Thomas, P. M. Harnsberger, F. P. Miknis, T. F. Turner, J. F. Branthaver, S-C. Huang, A. T. Pauli, D. A. Netzel, T. M. Bomstad, M. J. Farrar, D. Sanchez, J. F. McKay, and M. McCann. "Fundamental Properties of Asphalts and Modified Asphalts II, Final Report, Volume I: Interpretive Report," Federal Highway Administration, Contract No. DTFH61-99C-00022, Chapters 5-7 submitted for publication, March 2006.

Steinfeld, J. I., J. S. Francisco, and W. L. Hase, 1999, Chemical Kinetics and Dynamics, 2nd Edition, Prentice-Hall, Inc, Upper Saddle River, NJ, pp. 163-165, 408-410.